Bulk Synthesis of Two-Dimensional Polymers: The Molecular Recognition Approach

S. I. Stupp,* S. Son, L. S. Li, H. C. Lin, and M. Keser

Contribution from the Departments of Materials Science and Engineering and Chemistry, Materials Research Laboratory, Beckman Institute for Advanced Science and Technology, University of Illinois at Urbana-Champaign, Urbana, Illinois 61801

Received August 5, 1994[⊗]

Abstract: This manuscript describes the bulk synthesis of shape persistent two-dimensional (2D) polymers using the self-assembly of rigid precursor molecules into bilayers. A precursor was synthesized with a structure that encodes for the necessary molecular recognition events to form bilayers with internal orientational order. These events include homochiral interactions and confine reactive functions to planes leading to covalent stitching of flat polymers. The resulting molecular objects have a monodisperse thickness of 5 nm and polydisperse planar dimensions on the order of hundreds or thousands of nanometers. One of the stiching reactions, the oligomerization of acrylate groups to form an all-carbon backbone, is catalyzed by the presence of dipolar stereocenters 13 atoms away from the double bond. These enantiomerically enriched stereocenters are substituted by nitrile groups which react to generate the second stitching backbone of the plate-shaped molecules. A computer simulation indicates that 2D polymers of molar mass in the range of millions can be formed with extremely short stitching backbones provided planar confinement of functions is achieved by molecular recognition events. "Bulk" syntheses of shape persistent 2D polymers which do not require external boundaries to confine monomers into 2D spaces may lead to many interesting advanced materials.

Introduction

Throughout this century polymer science has studied the linear chain and its architectural derivatives which include familiar structures such as the branched chain and the three-dimensional network. As synthetic methodologies have become more sophisticated and new concepts of polymer structure invented, other derivatives have been added to the scope of the field such as rings,[1] ladders,[2] combs,[3] stars,[4] and dendrimers.[5] Most of the theories and synthetic methodologies in polymer science revolve around the concept of a one-dimensional covalent backbone, and most of the technical concepts related to polymeric materials, in use or under development, envision microstructures formed by entangled, aligned, or folded linear chains. One of the characteristic features of linear chain macromolecules that form ordered structures is a drastic change in shape, that is, conformation, as they pass from liquid to solid states. Two examples are the folding of linear chain coils into thin crystals when polymeric liquids solidify and the extension of globular coils in the preparation of solid fibers from the melt or solution. Our objective here is to depart from the focus on linear chains and explore the synthesis and properties of polymer molecules that can be considered *molecular objects*. Ideally, molecular object polymers would be composed of molecules with well-defined and persistent shapes that survive state transformations from neat liquids or solutions to the solid state and vice versa. These objects must also be of finite dimension and not form infinite, macroscopic structures.

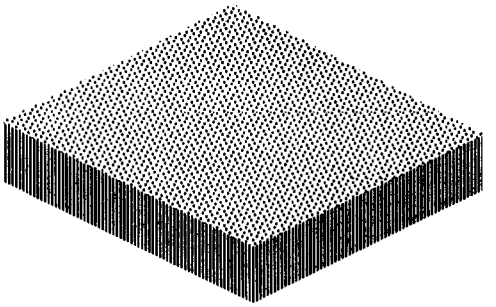

Figure 1. Schematic representation of a 2D polymer.

Shapes that are particularly interesting for molecular objects are those not common in the conformational space of linear chains, for example, two-dimensional (2D) objects shaped as sheets, and also macromolecular bundles shaped as disks, cylinders, parallelepipeds, or ellipsoids. The molecular object of interest in this paper is a 2D polymer with planar dimensions greater than its thickness and a shape-granting skeleton built by covalent bonds. This type of molecular object is depicted schematically in Figure 1. The ideal 2D polymer object is one with planar dimensions that are 1 or several orders of magnitude greater than its thickness. Thus depending on aspect ratio, such objects will have either weak or strong two-dimensionality. With regard to the shape-granting skeleton, one stabilized by covalent bonds would be ideal; however, weaker bonds such as hydrogen bonds could in principle participate in defining the shape of the object. Several groups have considered the physical properties and structure of 2D macromolecular structures theoretically,[6] and the work by Nelson and co-workers on thin polymerized membranes (often referred to as tethered membranes) has been particularly interesting.

[⊗] Abstract published in *Advance ACS Abstracts*, April 1, 1995.

(1) Brown, J. F., Jr.; Slusarczuk, G. M. *J. Am. Chem. Soc.* **1960**, *82*, 775. Geiser, D.; Höcker, H. *Macromolecules* **1980**, *13*, 653.

(2) Schlüter, A.-D. *Adv. Mater.* **1991**, *3*, 282. Arnold, F. E.; Van Deusen, R. L. *J. Appl. Polym. Sci.* **1971**, *15*, 2035.

(3) Rehberg, C. E.; Fisher, C. H. *J. Am. Chem. Soc.* **1944**, *66*, 1203. Shibaev, V. P.; Kozlovsky, M. V.; Beresnev, L. A.; Blinov, L. M.; Platé, N. A. *Polym. Bull.* **1984**, *12*, 299.

(4) Roovers, J.; Zhou, L. L.; Toporowski, P. M.; Vanderzwan, M.; Iatrou, H.; Hadjichristidis, N. *Macromolecules* **1993**, *26*, 4324. Ishizu, K.; Yukimasa, S. *Polymer* **1993**, *34*, 3753.

(5) Tomalia, D. A.; Naylor, A. M.; Goddard, A., III. *Angew. Chem., Int. Ed. Engl.* **1990**, *29*, 138. Hawker, C. J.; Fréchet, J. M. J. *J. Am. Chem. Soc.* **1990**, *112*, 7638. Miller, T. M.; Neenan, T. X. *Chem. Mater.* **1990**, *2*, 346.

0002-7863/95/1517-5212$09.00/0 © 1995 American Chemical Society

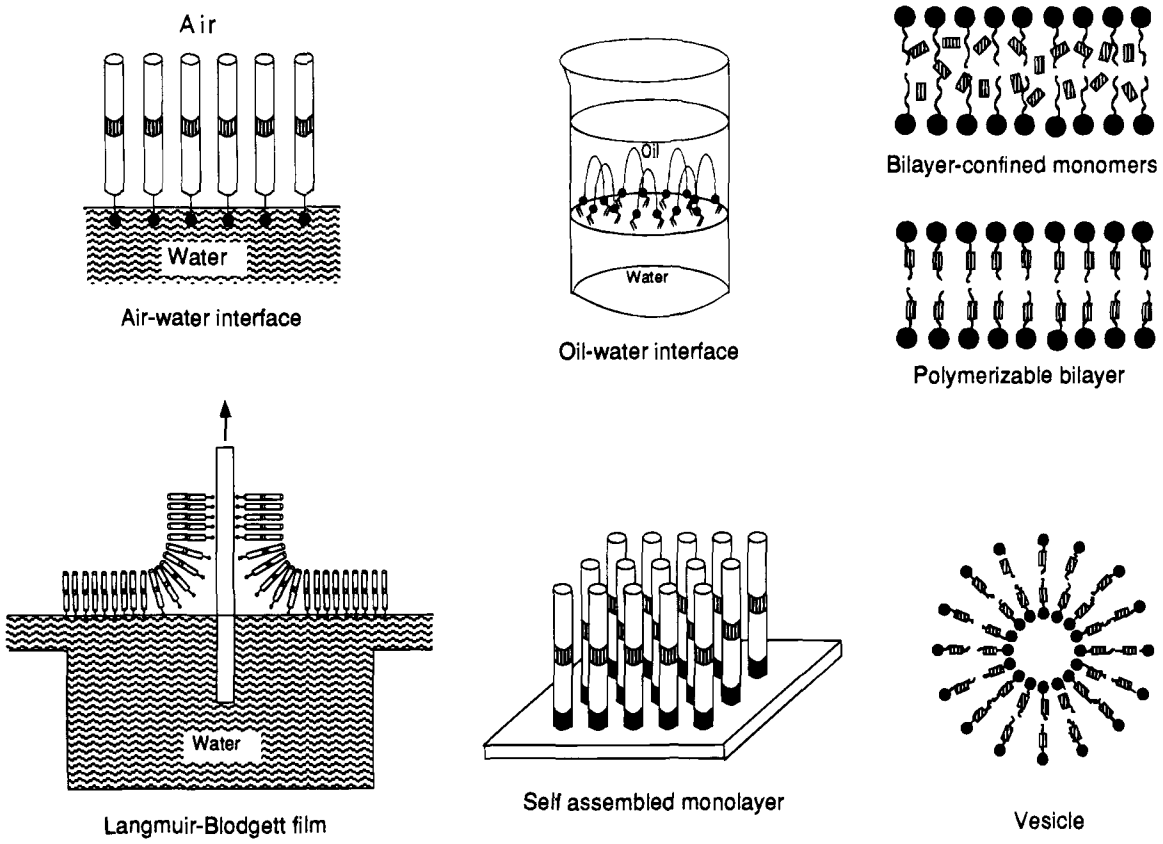

Figure 2. Approaches to the confinement of monomers into 2D spaces for 2D polymerization.

Experimental work has involved the properties of systems such as polymerized lipids,[7] graphite oxide membranes,[8] and networks formed at oil–water interfaces.[9] Theoretical efforts on the "fish net" structures have predicted the existence of flat phases,[10] crumpled phases,[11] and folding transitions that precede compact phases at low temperatures.[12] Predictions of flat macromolecules and folding transitions are intriguing for concepts in advanced materials and will have to be verified as synthetic chemistry generates new structures. The physical behavior of internally anisotropic 2D polymers considered here, with thicknesses on the order of 100 atoms, may differ from those envisioned in theoretical work. This remains an open and interesting question for the future.

The availability of molecular objects with well-defined shape and finite size could have profound consequences in the production of materials. One example with 2D polymers is the possibility of developing bulk materials with self-organized surfaces resulting from the macroscopic stacking of these molecular objects. Such materials could spontaneously generate during processing the chemically defined surfaces of Langmuir–Blodgett films or self-assembled monolayers. This would be of great significance in the reliable preparation of films, fibers, or particles with stable sensor or adhesive surfaces. Two-dimensional polymers could also be used to molecularly reinforce linear polymers, create more durable structures, or entrap particles through their folding transitions. The use of polymeric molecular objects as materials might only be feasible if methodologies are developed to synthesize them through "bulk" reactions. This means the use of monomers that will undergo spontaneous molecular organization into the desired shapes in the absence of surfaces, dispersing media, solvents, or external forces. The instructions for precursor molecules to self-organize and react must be encoded in their chemical structure. Chemical reaction would follow to achieve covalent stitching among the monomers and thus transform the assembly into an object of persistent shape. This chemical reaction may not be necessary or sufficient to reach the synthetic goal. The current manuscript describes our first effort in constructing a 2D polymer object through a bulk reaction. The work described here is a more detailed account of our initial report on the subject.[13]

Previous investigators considered molecular structures that have some resemblance to the 2D polymers of interest here. Synthetic work has been primarily related to the polymerization of amphiphiles that form layered structures when dispersed in water[14] and the formation of infinite 2D networks at oil–water interfaces.[15] Other synthetic work focused on the related phenomenon of 2D polymerization.[16] As Figure 2 illustrates,

(6) Mori, S.; Wadati, M. *J. Phys. Soc. Jpn.* **1993**, *62*, 3864. Kantor, Y.; Kremer, K. *Phys. Rev. E* **1993**, *48*, 2490. Morse, D. C.; Petsche, I. B.; Grest, G. S.; Lubensky, T. C. *Phys. Rev. A* **1992**, *46*, 6745. Abraham, F. F.; Kardar, M. *Science* **1991**, *252*, 419. Abraham, F. F.; Nelson, D. R. *Science* **1990**, *249*, 393. Abraham, F. F.; Nelson, D. R. *J. Phys. (Paris)* **1990**, *51*, 2653.

(7) Eggl, P.; Pink, D.; Quinn, B.; Ringsdorf, H.; Sackmann, E. *Macromolecules* **1990**, *23*, 3472.

(8) Wen, X.; Garland, C. W.; Hwa, T.; Kardar, M.; Kokufuta, E.; Li, Y.; Orkisz, M.; Tanaka, T. *Nature* **1992**, *355*, 426.

(9) Rehage, H.; Veyssié, M. *Angew. Chem.* **1990**, *102*, 497.

(10) Abraham, F. F.; Nelson, D. R. *Science* **1990**, *249*, 393. Abraham, F. F.; Nelson, D. R. *J. Phys. (Paris)* **1990**, *51*, 2653.

(11) Kantor, Y.; Kardar, M.; Nelson, D. R. *Phys. Rev. Lett.* **1986**, *57*, 791.

(12) Abraham, F. F.; Kardar, M. *Science* **1991**, *252*, 419.

(13) Stupp, S. I.; Son, S.; Lin, H. C.; Li, L. S. *Science* **1993**, *259*, 59.

(14) Hub, H.; Hupfer, B.; Koch, H.; Ringsdorf, H. *Angew. Chem., Int. Ed. Engl.* **1980**, *19*, 938. Dorn, K.; Klingbiel, R. T.; Specht, D. P.; Tyminski, P. N.; Ringsdorf, H.; O'Brien, D. F. *J. Am. Chem. Soc.* **1984**, *106*, 1627. Sakada, K.; Kunitake, T. *Chem. Lett.* **1989**, 2159. Asakuma, S.; Okada, H.; Kunitake, T. *J. Am. Chem. Soc.* **1991**, *113*, 1749. Kuo, T.; O'Brien, D. F. *Langmuir* **1991**, *7*, 584. Gros, L.; Ringsdorf, H.; Schupp, H. *Angew. Chem., Int. Ed. Engl.* **1981**, *20*, 305. Fendler, J. H.; Tundo, P. *Acc. Chem. Res.* **1984**, *17*, 3.

(15) Rehage, H.; Schnabel, E.; Veyssié, M. *Makromol. Chem.* **1988**, *189*. 2395. Dubault, A.; Casagrande, C.; Veyssie, M. *J. Phys. Chem.* **1975**, *79*. 2254.

Scheme 1

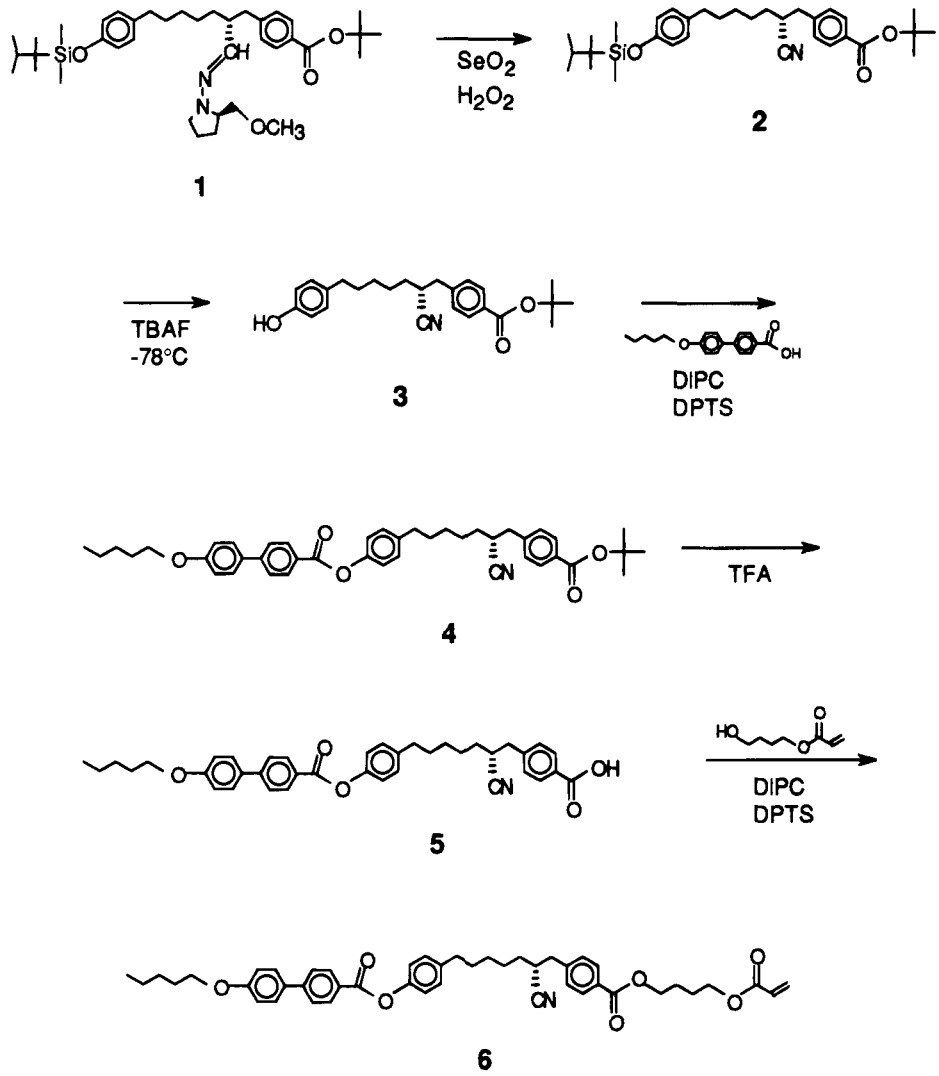

1 2 3 4 5 6

in a 2D polymerization monomers are confined to a 2D space using various types of boundaries. The confining environment may be created by an oil–water interface,[17] the air–water interface of a Langmuir trough,[18] the solid surface that organizes a self-ordered monolayer,[19] or the interior of a lipid or surfactant bilayer surrounded by water.[20] In fact in this last case the lipid or surfactant molecules might be the monomers themselves. Once in 2D confinement monomers polymerize, but synthesis of a finite 2D polymer is not necessarily achieved unless the monomers have more than one polymerizable function and their structures are molecularly rigid. Without monomeric rigidity and strong bonds among the monomers, removal of the confining boundary will lead to the collapse of the incipient 2D object to the characteristic globular shape of polymer molecules. This would occur readily in solution or at high temperature, and therefore a shape persistent 2D polymer that survives state transformations is not necessarily formed by a 2D polymerization. In the event that monomers are not monofunctional and that the rigidity requirement is met, a true 2D polymer could form. However, since confining boundaries are key elements in previously studied systems, we would not be able to classify them as "bulk syntheses" of 2D polymers. This is the case of amphiphiles that must be dispersed in water and exposed to sonication in order to form layered assemblies or vesicular structures which are not globally two-dimensional. Water molecules bound to ionic groups form the confining boundary in these systems.

This manuscript studies a methodology that may be used to construct 2D polymers through a bulk reaction. The synthesis of the precursor and the product are described as well as their characterization by techniques such as electron diffraction, electron microscopy, gel permeation chromatography, and differential scanning calorimetry. We also use a computer simulation to estimate the extents of reaction necessary to form large 2D polymers and to illustrate the importance of molecular recognition events in their synthesis.

Results and Discussion

Molecular Design and Recognition. As stated before, the precursor molecule for bulk synthesis of 2D polymers must have encoded in its chemical structure instructions to self-organize into reactive assemblies. In this work we investigated precursor **6** synthesized through a 21-step pathway partly described in Scheme 1. The ideal assembly that **6** must form in order to create a planar molecular object must satisfy a number of requirements, and it is depicted at the top of Figure 3. First of all, its constituent molecules must have more than one reactive group for catenation reactions, in this case, acrylate and nitrile groups. If the assembly were to contain only one such group,

(16) Sakada, K.; Kunitake, T. *Chem. Lett.* **1989**, 2159. Asakuma, S.; Okada, H.; Kunitake, T. *J. Am. Chem. Soc.* **1991**, *113*, 1749.
(17) Rehage, H.; Schnabel, E.; Veyssié, M. *Makromol. Chem.* **1988**, *189*, 2395.
(18) Day, D.; Hub, H.-H.; Ringsdorf, H. *Isr. J. Chem.* **1979**, *18*, 325.
(19) Wu, J.; Harwell, J. H.; O'Rear, E. A. *Langmuir* **1987**, *3*, 531.
(20) Regen, S. L.; Shin, J.-S.; Yamaguchi, K. *J. Am. Chem. Soc.* **1984**, *106*, 2446.

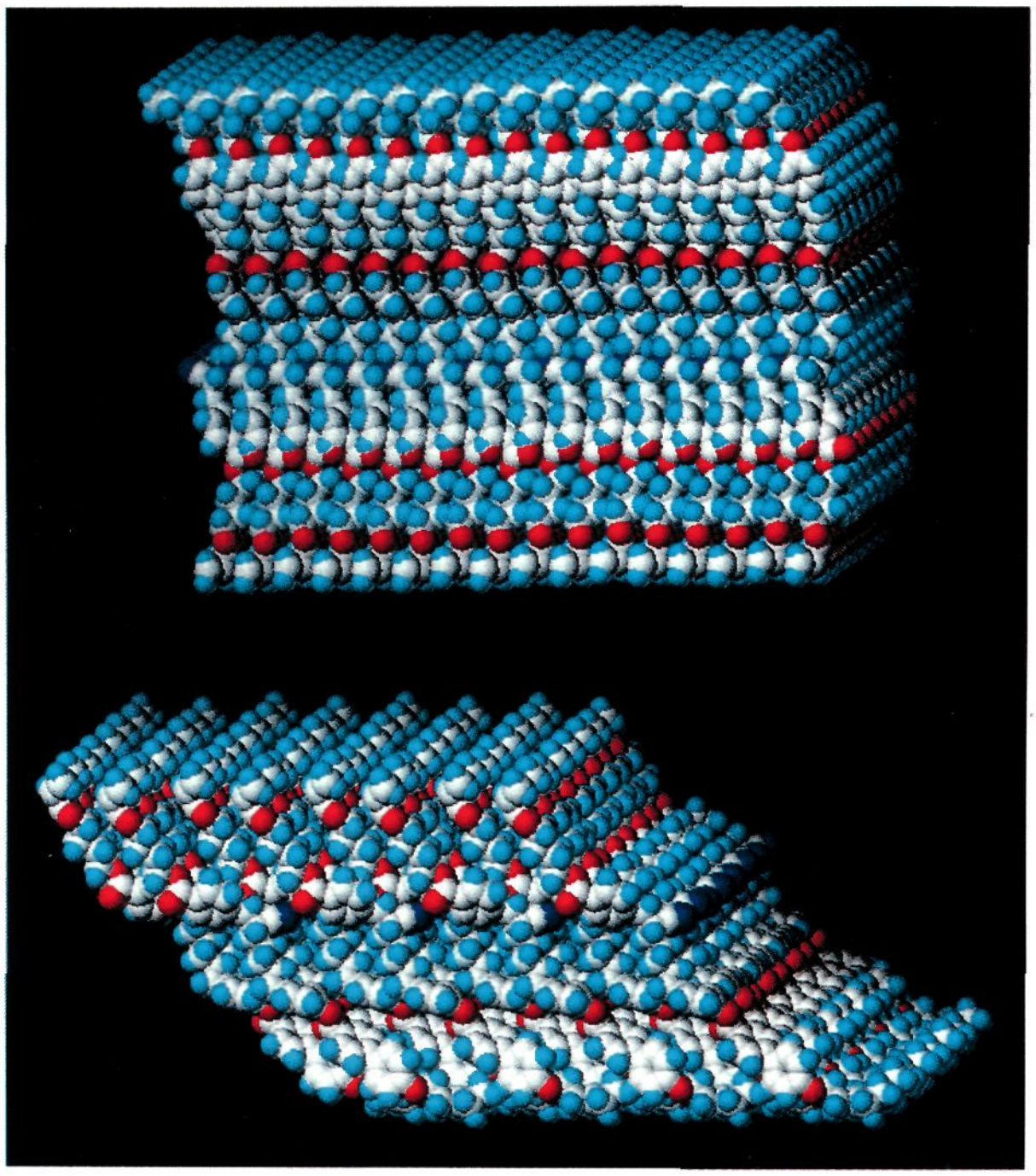

Figure 3. Computer-generated renditions of layered assemblies of precursor molecules. The bottom assembly contains molecules tilted relative to the layer normal (see text).

it would form the architectural derivative of the linear chain known as a comb polymer. Having two functions it is possible in principle to catenate the oligomeric precursor into a sheet. Second, if molecules in the precursor assembly lack $D_{\infty h}$ symmetry, they must have the orientational order required to confine the reactive functions in distinct planes of the layer. If this were not the case, the stitching reactions would not be very effective in forming large molecular objects and two-dimensionality would not arise. This point is supported later in the manuscript through the use of computer simulation. A possible advantage of not using precursor molecules with $D_{\infty h}$ symmetry is to avoid high melting points, thus favoring the formation of thermodynamically stable layered mesophases in which reactions can take place. Third, the two distinct planes of functions must be far enough apart to avoid the correlation of polymerizing paths, otherwise 1D ladder polymers would form. Finally, at least one surface of the layered assembly must be free of reactive functions, otherwise the product would be an infinite network (an insoluble polymeric gel). This violates our objective of forming molecular objects of finite dimension. When the layered assembly is free of functions on either surface, the planar object has monolayer character but becomes a bilayer 2D polymer when one surface contains reactive groups. The assembly shown in Figure 4 is therefore expected to form bilayer 2D polymers.

The instructions in precursor **6** to form layers can be provided in part by its alkoxybiphenyl terminus, a well-known smectogenic segment.[21] Interactions such as $\pi-\pi$ overlap of biphenyl units may contribute to the molecular recognition events that result in layered assemblies. Molecular recognition events are also important in forming an orientationally ordered assembly, and in principle, this organization could be encoded by homochiral interactions among stereocenters. In precursor **6** this effect should be particularly strong given the large dipole moment of nitriles and thus a significant energy associated with their ferroelectric ordering. In fact, calculations by Andelman and DeGennes[22] predict a preference for homochiral recognition for chiral molecules in which dipole moments or full charges are associated with stereocenters. The calculations were inspired by the possibility of predicting surface segregation of chiral, surfactant molecules as a result of preferences for homochiral vs heterochiral interaction. The molecules of their model were tripod-shaped and contained a stereocenter at the base. The three substituents of the stereocenter, other than the hydrophobic tail, occupy corners of a triangle as shown schematically in Figure 5. The calculation predicts that Δ, the difference between partition functions for heterochiral, Z_{DL}, and homochiral interaction, Z_{DD}, is always greater than zero when two substituents have dipoles or charges and the third is apolar. Therefore, a preference for homochiral interaction is predicted for this case. In previous work in our group,[23] the methine proton of **6** was

(21) Gray, G. W.; Hartley, J. B.; Jones, B. *J. Chem. Soc.* **1955**, *236*, 1412.

(22) Andelman, D.; DeGennes, P. G. *C. R. Acad. Sci. Ser. II* **1988**, *307*, 233.

(23) Moore, J. S.; Stupp, S. I. *J. Am. Chem. Soc.* **1992**, *114*, 9.

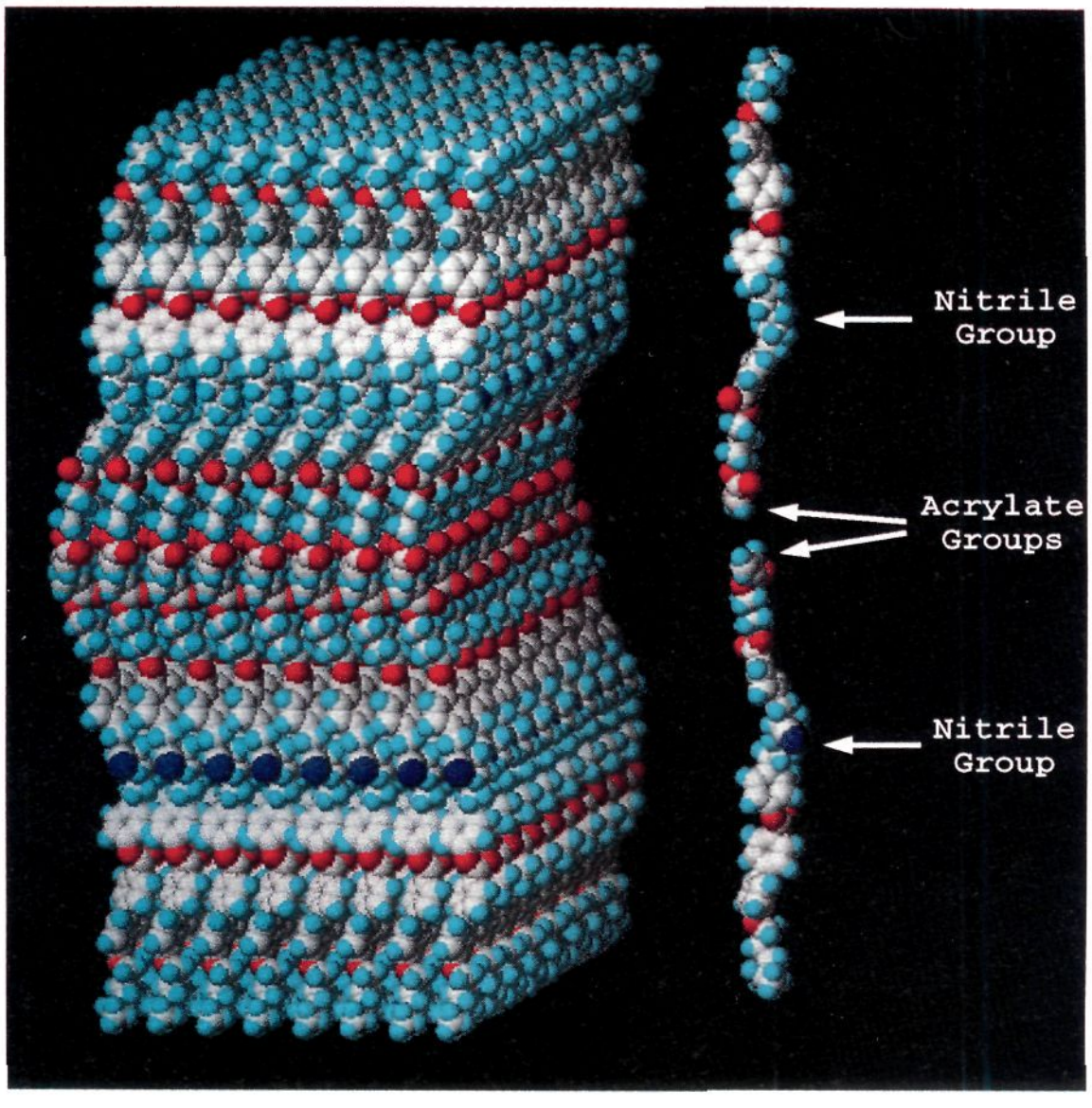

Figure 4. Computer-generated rendition of a small sector of an orientationally ordered bilayer that can serve as the precursor assembly of 2D polymers.

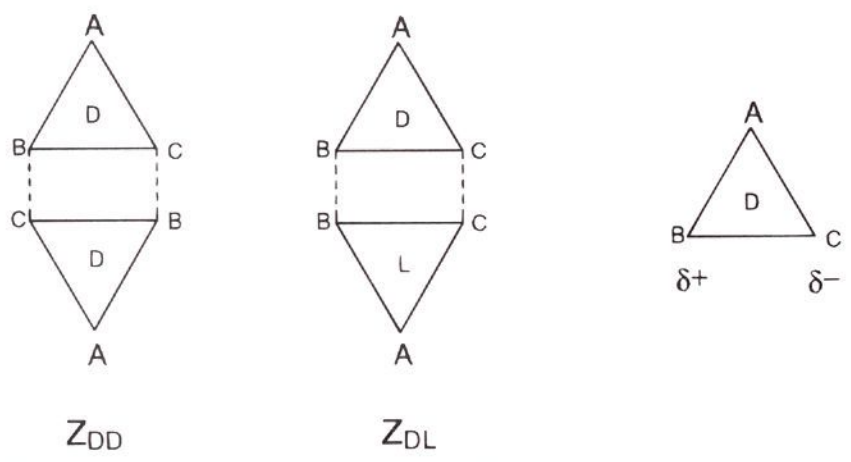

Figure 5. Schematic representation of homochiral and heterochiral interactions between two interacting dipolar stereocenters at the base of a tripod-shaped molecule (see text, after Andelman and DeGennes, 1988).

found to be acidic, and thus it is reasonable to classify in this category the stereocenter of precursor molecule **6**:

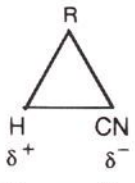

$$\Delta = Z_{DD} - Z_{DL} > 0$$

where Δ is a function of the interaction energies F_{RR}, F_{HH}, F_{CNCN}, F_{RH}, F_{HCN}, and F_{RCN}. The required separation between functional planes in a layered assembly of **6** is provided by the butoxy ester spacer and the benzylic fragment separating reactive groups. As explained before, this separation of functional planes is necessary to avoid the formation of ladder polymers.

Characterization of Experimental System. Evidence for layering of **6** is offered by the optical textures characteristic of smectic phases observed upon examination of **6** by hot stage polarized optical microscopy. One example of these textures was shown in our earlier publication.[13] Figure 6 shows at the top an electron micrograph of **6** at room temperature providing unequivocal evidence for the existence of layered structures in this compound. Figure 6 also shows the small angle electron diffraction pattern which indicates that molecules are organized into layers measuring 303 Å in thickness. The wide angle electron diffraction pattern can be indexed if the unit cell is assumed to be monoclinic (see Figure 7). We therefore believe the layers of **6** at room temperature contain molecules tilted relative to the layer normal. Diffraction data in an oligomeric material analogous to **6**, in which we were able to obtain an appropriate sample,[24] reveal a tilt angle of 34.8°. If we assume that molecules in **6** are similarly tilted and have a fairly extended conformation, the thickness of 303 Å corresponds to eight molecular layers. The bottom of Figure 3 depicts by molecular graphics a layer of tilted molecules of **6** packed in the monoclinic unit cell of the analogous compound. It is not clear to us at this time why molecules of **6** self assemble into "octalayers". However, given the fiber-like wide angle electron diffraction pattern, it is possible the layers are twisted with a 303 Å period of revolution. The tilted structures are observed of course at low temperatures, but the reactive assemblies at high temperature might be more accurately depicted by the orthogonal assembly at the top of Figure 3.

The bottom of Figure 6 shows electron micrographs of the bilayer flat objects observed after **6** is heated to 125 °C for 20 h. The 2D polymers formed are always stacked parallel to the glass substrate on which they are formed when specimens are prepared for electron microscopy. An interesting characteristic of the stacked 2D structures is their single-crystal nature at room temperature.[13] Stacked layers are also formed by a 1D isomer

(24) Li, L. S.; Stupp, S. I. Submitted for publication.

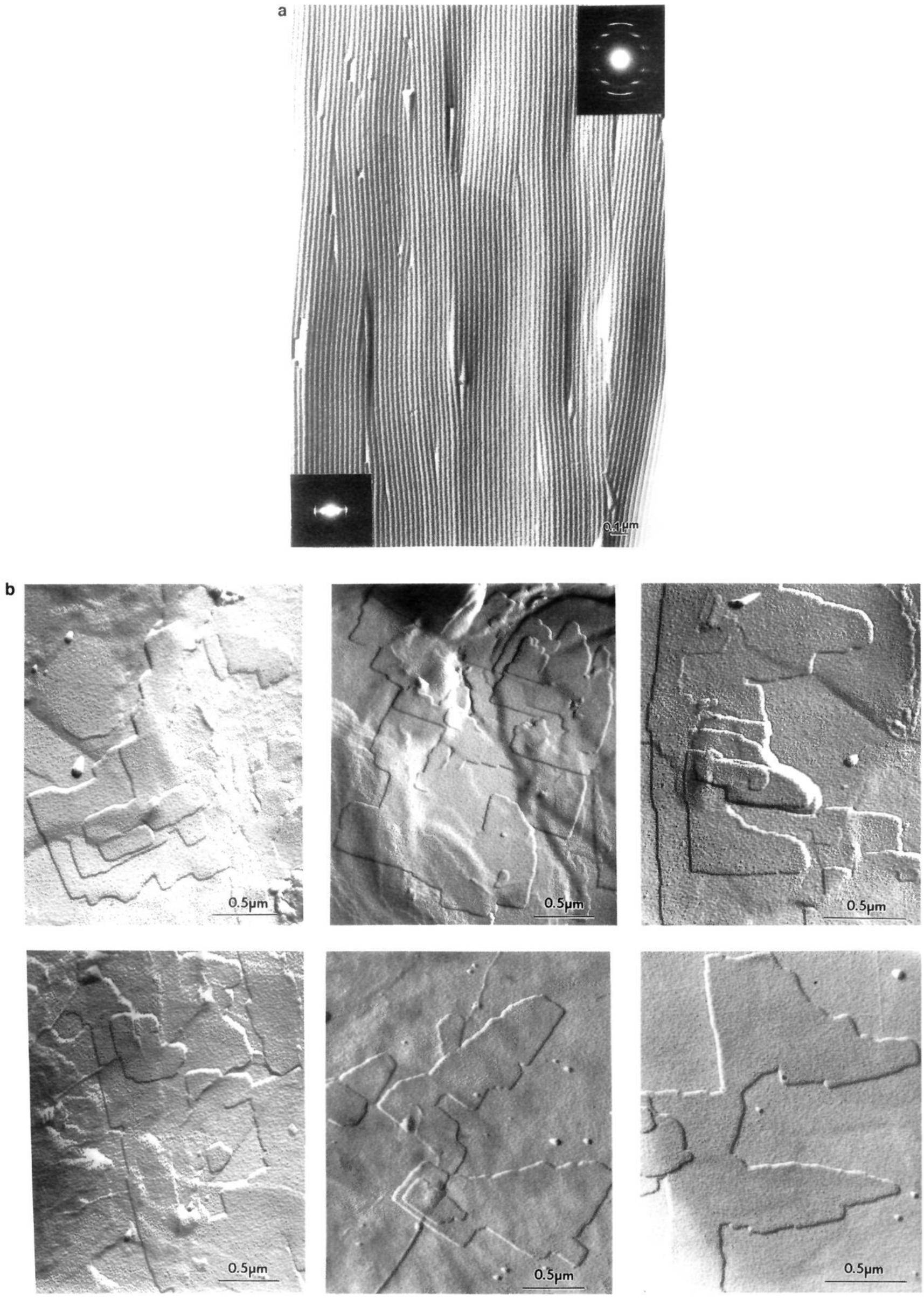

Figure 6. (a) Transmission electron micrograph of **6** at room temperature revealing its self-assembly into a layered structure. Small angle and wide angle electron diffraction patterns are shown in the lower left and upper right corners, respectively. (b) Transmission electron micrographs of the product obtained after **6** is heated to 125 °C for 20 h.

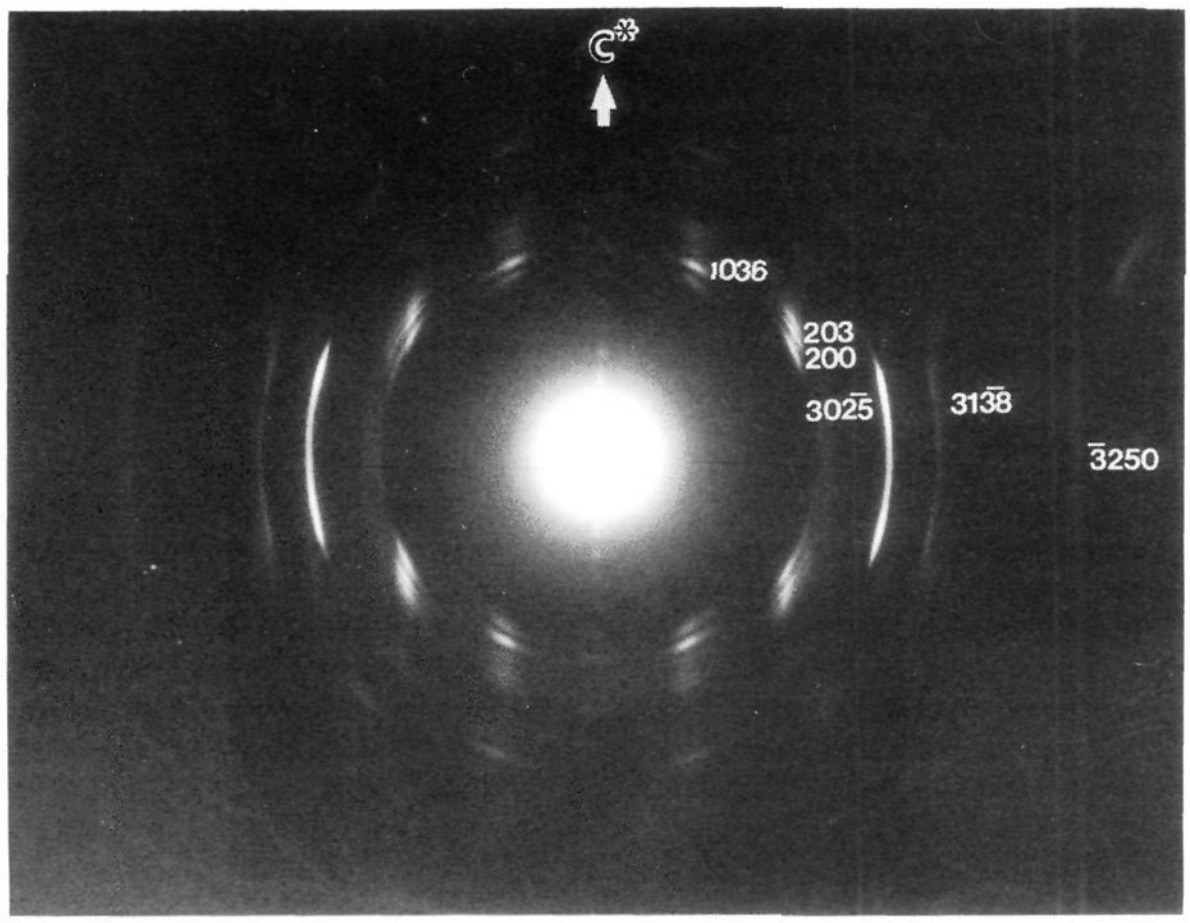

Figure 7. Wide angle electron diffraction pattern of the 2D polymer's precursor compound.

of the 2D polymer synthesized by dilute solution free radical polymerization.[13] However, the single-crystal stacks are *never* observed in the 1D comblike polymer. Instead, one observes a structure analogous to a smectic E mesophase with cooperative rotation of the smectogens making up the layers.[24] We view this fundamental difference as a direct consequence of 2D covalent architecture in the product. The smectic E-like structure is observed in some regions of the 2D polymer product, possibly revealing local variations in architecture or degree of reaction. Interestingly, the molecular axis of precursor segments in the single-crystal stacks of 2D polymers is parallel to the layer normal. In other words, the tilt in precursor molecules discussed above is not observed after the polymerization reaction. Thus, as suggested previously, the orthogonal assemblies depicted in Figure 3 might prevail at high temperatures when polymerization occurs.

We reported earlier a characteristic thickness of 50.2 Å for 2D polymers stacked in the solid state, measured by X-ray diffraction. This thickness is significantly smaller than that expected if precursor molecules existed in an extended conformation within the bilayer 2D polymer (~92 Å). The experimental fact is that a high degree of order exists within these 2D polymers, and as mentioned above, we observe the assembly of single-crystal stacks in these structures. Analysis of electron diffraction data indicates the unit cell is orthorhombic and contains four precursor molecules per cell, and its lattice parameters are $a = 8.38$ Å and $b = 10.56$ Å. After considering many molecular models and both the X-ray and electron diffraction data, we believe the thickness of 50.2 Å is the result of interdigitation between the rodlike termini of precursor molecules in adjacent bilayer 2D polymers. This idea is depicted in the molecular graphics rendition of Figure 8. This figure shows interdigitated precursor molecules that would belong to two adjacent 2D polymer molecules. The molecular segments are packed in an orthorhombic unit cell using experimental lattice parameters. We also envision that conformational disorder exists in reactive segments at the center of 2D polymer molecules (nonextended segments in Figure 8). The molecular conformations used in Figure 8 were generated as follows. The stiff portion of the molecule was frozen, and a high-temperature molecular dynamics run was used to generate thousands of conformations. We selected eight conformers from this pool, minimized their energies, and used them to generate the figure. As indicated in the figure, the model would be consistent with the long period of 50.2 Å observed by X-ray diffraction. We do not know at this time if segmental interdigitation would precede the chemical reactions or if it is a consequence of polymerization. The model suggests formation of interesting molecules once bilayers become dislodged from each other in a solvent. A great deal of surface area for interaction with solvent could exist when the rodlike termini of molecular precursors are tethered to a disordered network in the middle of the bilayer 2D polymer.

Figure 9, top, shows the differential scanning calorimetry (DSC) scan of **6** revealing the various phase transitions of the monomer. The highest temperature transition of **6** transforms a smectic phase to an isotropic phase (nonbirefringent phase) at 98 °C. This smectic phase is most likely the positionally disordered smectic A phase on the basis of diffraction experiments in our laboratory on other similar compounds. The reactions that catenate oligomers into 2D objects are, of course, exothermic, and their calorimetric signature emerges as an exotherm in the DSC spectrum above the isotropization transition. If one observes by optical microscopy precursor **6** as it nears the isotropization transition, one observes that birefringence disappears almost entirely but a small amount remains in the field of view. This implies that self-ordering of molecules into smectic phases occurs as the catenating chemical reactions commence. It also implies that the chemical reaction begins below the isotropization transition of the precursor assembly. It is well known that isotropization transitions of smectic phases increase when oligomerization of the smectogen occurs.[25] As catenation takes place, specific volume will decrease and higher transition temperatures are expected. However, an orderly polymerization proceeds above the isotropization transition and not the formation of an amorphous gel, suggesting that molecular recognition events among monomers play a key role in the transformation of **6** to 2D polymers. Within a few minutes isotropic regions observed by optical microscopy become fully birefringent when held isothermally at 110 °C.

(25) Percec, V.; Lee, M. *Macromolecules* **1991**, *24*, 2780.

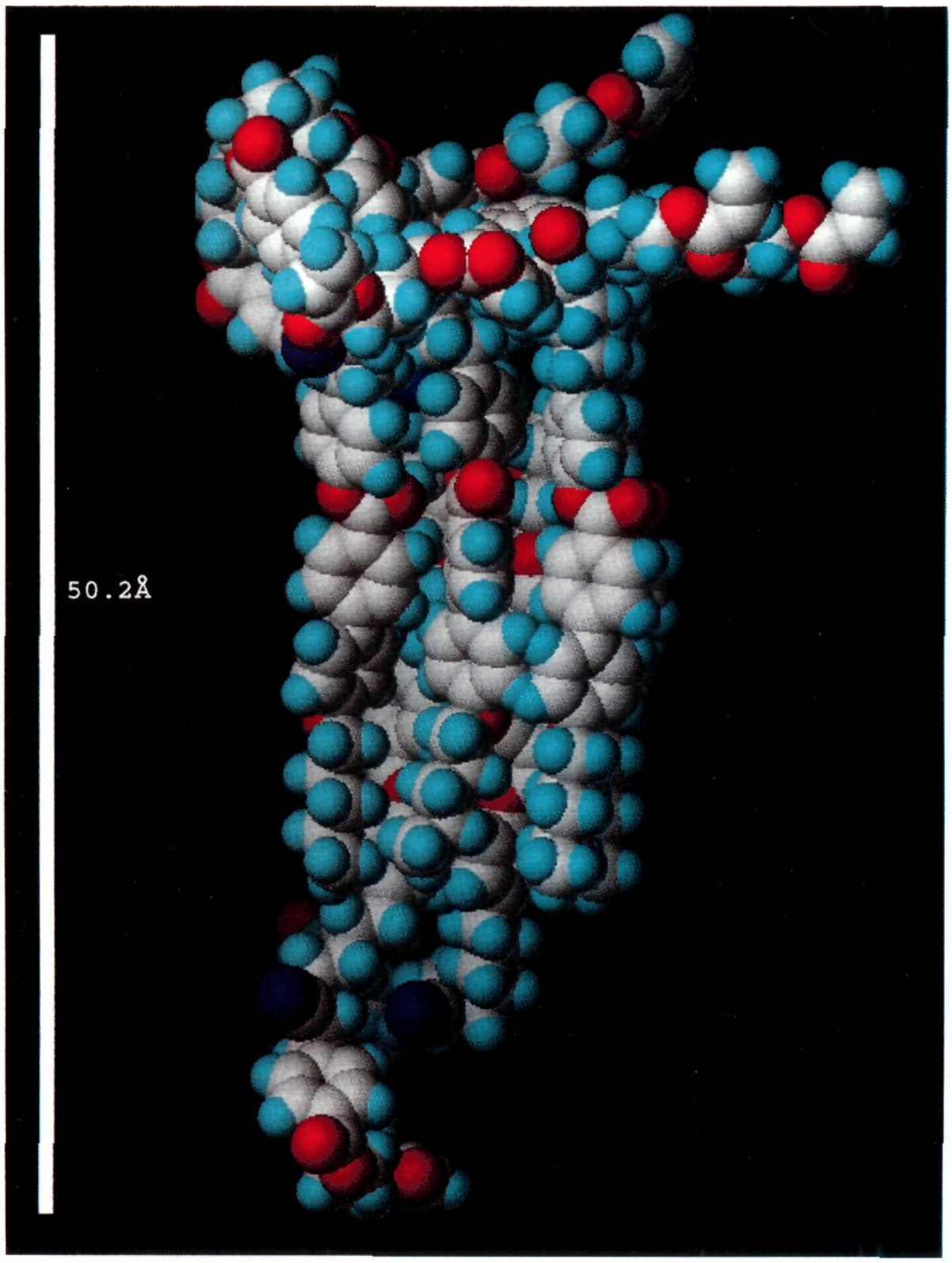

Figure 8. Computer-generated model for the interdigitation of molecular segments in adjacent 2D macromolecules.

Enantiomeric enrichment was found to affect the transformation of the compound upon heating. Enantiomeric excess values were measured using chiral shift reagents following a method described in one of our previous publications.[13] Interestingly, the racemate did not appear to react easily and remained mostly isotropic at temperatures and times when the enantiomer would have retransformed fully to a liquid crystalline phase. As the racemate was heated above its isotropization temperature,[26] a biphasic fluid containing both birefringement and nonbirefringent regions was observed over the temperature range of 150–220 °C. The phase transitions of the racemate below 100 °C were similar to those observed in the enantiomerically enriched compound. Interestingly, however, the onset of the exotherm in the racemate was observed near 155 °C, approximately 28 °C above the onset of **6** (the DSC scan of the racemate is shown in Figure 9, bottom). These observations suggest that the chemical reactions taking place are sensitive to the relative stereochemistry of nitrile groups. Specifically, the DSC data indicate that acrylate group polymerization does not take place as easily in the racemate as it does in the enantiomerically enriched compound. Furthermore, observations on achiral compound **12** (see Scheme 2) suggest that this difference is not simply the result of better molecular packing in the enantiomerically enriched compound relative to the racemate. Compound **12** which lacks the nitrile group has a higher isotropization temperature than either **6** or the racemate (115 °C vs 98 °C) and should therefore exhibit the most efficient packing. However, isothermal DSC experiments measuring heat evolved due to acrylate polymerization, Q, as a function of time indicate clearly that compound **12** reacts more slowly than **6**. The heat contributed by reaction among nitrile groups would be negligible compared to that associated with acrylate polymerization. The slower reaction in **12** is revealed by graphs in Figure 10 which plot the extent of reaction, P, as a function of time, t, at 150 °C in samples **6** and **12**.

$$P = \frac{\int_{t=0}^{t} (\mathrm{d}Q/\mathrm{d}t)\mathrm{d}t}{Q_{\text{total}}} \tag{1}$$

Varying the temperature of the experiment, the rate of reaction, R, obtained from the slope of curves in Figure 10 can be fitted

(26) The racemate's isotropization temperature was observed at 101.8 °C with an onset at 99.6 °C.

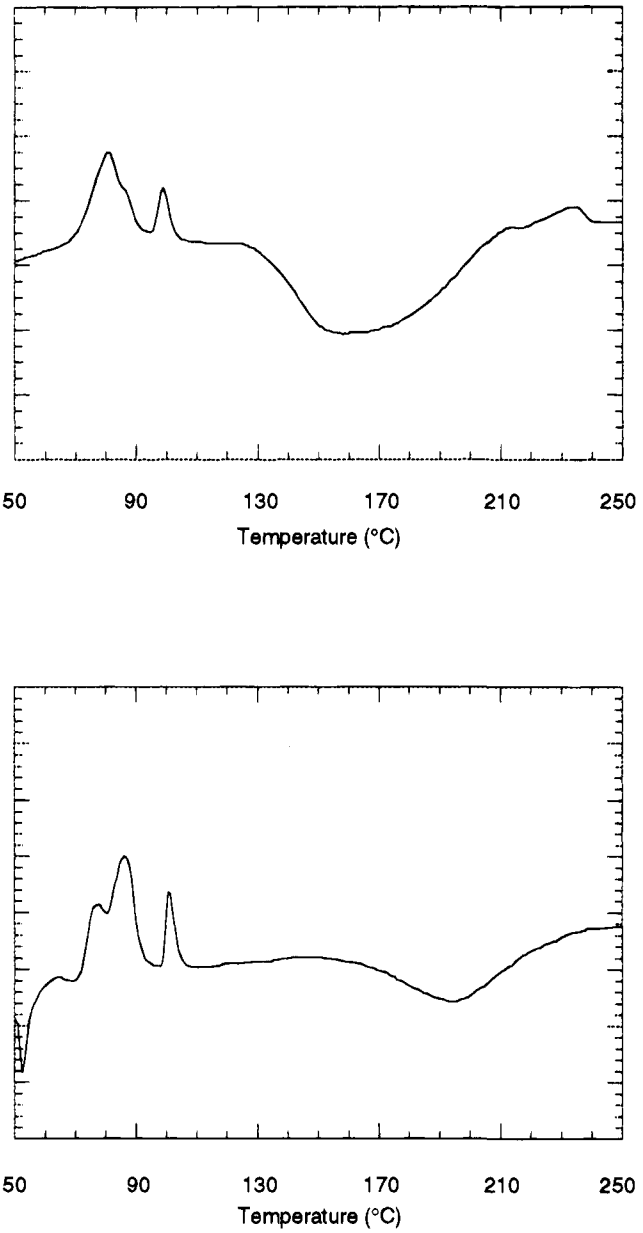

Figure 9. Differential scanning calorimetry scans of **6** (top) and its corresponding racemate (bottom). Both scans reveal multiple phase transitions and the exotherm associated with 2D polymer stitching reactions. The onset of the racemate's exotherm is shifted to a higher temperature.

within a given range of P to eqs 2 and 3 corresponding to compounds **6** and **12**, respectively,

$$R = B \exp(-\Delta E/kT) \exp(-2P) \quad (2)$$

$$R = A \exp(-\Delta E'/kT) \quad (3)$$

The fit to eq 2 for compound **6** holds for $P < 0.9$, and that to eq 3 for compound **12** holds in the range $0.15 < P < 0.85$. It is clear from these fits that differences exist in the reaction mechanism for the chiral and achiral compounds. The absence of an induction period in the chiral compound suggests that molecules are preorganized in assemblies that facilitate reaction. We therefore believe homochiral recognition in **6** catalyzes the addition of double bonds to form a poly(acrylate) backbone. It would then be reasonable to suggest that this polymerization is catalyzed by the homochiral interaction of nitriles 13 atoms away from the double bond.

Spectroscopic evidence for the chemical reactions was obtained by infrared spectroscopy as well as ^{1}H and ^{13}C NMR. After **6** has been kept at 140 °C for 14 h under a nitrogen atmosphere, the infrared spectrum reveals the consumption of 30−50% of the nitrile groups. ^{1}H and ^{13}C NMR spectra reveal that double bonds have essentially disappeared, and we infer from these observations that at least 90% of the acrylate groups have reacted. After the chemical reaction the ^{1}H NMR spectrum also reveals shifts in the benzylic and methine proton resonances of **6**. The largest shift is observed for benzylic protons β to the nitrile α carbon. The spectroscopic changes observed after reaction are shown in Figure 11. In the ^{13}C NMR spectrum we observed the resonance corresponding to the nitrile carbon of **6** at 121.4 ppm, as well as that of the methine carbon in the poly(acrylate) backbone. The spectroscopic data are consistent with acrylate polymerization as well as partial reaction of nitrile groups. The sharpness of NMR signals in the 2D polymer may be the result of different factors. First of all, the average degree of polymerization in individual stitching backbones may be quite low. Thus, local motions could be very different from those in an ordinary 1D polymer in which thousands of monomers may be connected through a single molecular backbone. Second, we expect the middle section of the bilayer to be a fairly disordered region relative to the outer sublayers containing rodlike segments. This middle section is therefore easily swollen by solvent in solution from lateral surfaces or through holes in the 2D structure left behind by unreacted monomer molecules or small clusters of reacted monomer molecules.

The reaction among nitriles in poly(acrylonitrile) at elevated temperatures leading to the formation of conjugated imine bonds is well known.[27] In this case the product is a ladder-like polymer resulting from the intramolecular reaction among nitriles. A similar reaction in **6** would result in intermolecular cross-linking within the layered assembly. We synthesized compound **13** through Scheme 3 in order to verify experimentally that a catenating reaction could occur in our system even in the absence of acrylate groups. This compound was found to be liquid crystalline and heated to 133 °C for 36 h below its isotropization transition (135 °C). This thermal treatment resulted in the appearance of a birefringent phase of higher isotropization temperature. On the basis of our previous discussion, this observation demonstrates the thermal oligomerization of **13** even though acrylate groups are no longer present. Samples also turn very pale yellow after reaction, and this color change is also observed in the transformation of poly(acrylonitrile) as a result of reaction among nitriles.[28] Given the intensity of the resonance corresponding to the methine carbon of the poly(acrylate) backbone in Figure 11, the rigidity of conjugated imine sequences, and the fact that only 30−50% of the nitriles are consumed, we infer that it is not possible to detect the imine carbon resonance in the ^{13}C NMR spectrum.

Nitrile polymerization is known as a high-temperature transformation, occuring at a significant rate near 200 °C. In our system consumption of nitriles appears to take place at relatively low temperatures, specifically within the range 110−150 °C. Our view is that enantiomeric enrichment of the stereocenter containing the nitrile group plays a role in the enhanced reactivity. A related previous observation is the finding that poly(acrylonitrile) with higher ratios of isotactic to syndiotactic diads exhibits a higher rate of reaction among nitrile groups.[29] Two other factors that may catalyze the nitrile reaction in our system are the prevailing order in the medium of the reaction and also the formation of the poly(acrylate) backbone

(27) Grassie, N.; NcNeil, I. C. *J. Chem. Soc.* **1956**, *3929*. Grassie, N.; McNeil, I. C. *J. Polym. Sci.* **1958**, *27*, 207. Turner, W. N.; Johnson, F. C. *J. Appl. Polym. Sci.* **1969**, *13*, 2073. Renschler, C. L.; Sylwester, A. P.; Salgado, L. V. *J. Mater. Res.* **1989**, *4*, 452.

(28) Grassie, N.; NcNeil, I. C. *J. Chem. Soc.* **1956**, *3929*.

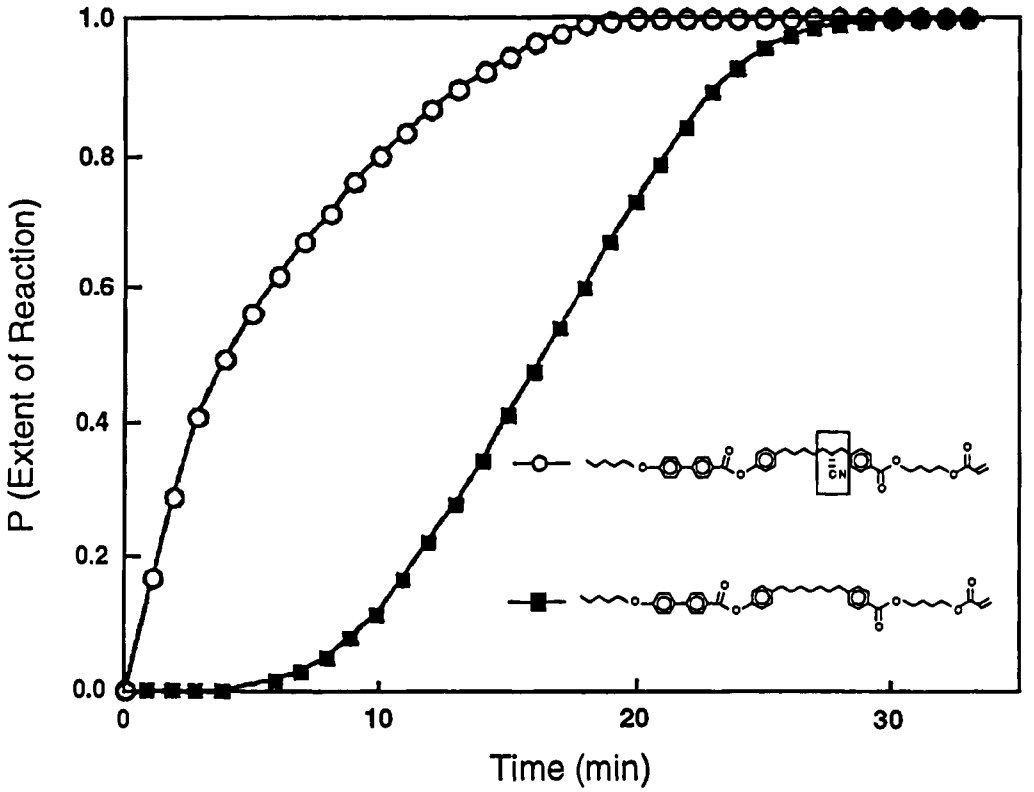

Figure 10. Isothermal plots of extent of reaction, *P*, as a function of time in compounds **6** and **12** obtained at 150 °C. The solid lines represent a fit of the data to eq 1 and 2 (see text).

Scheme 2

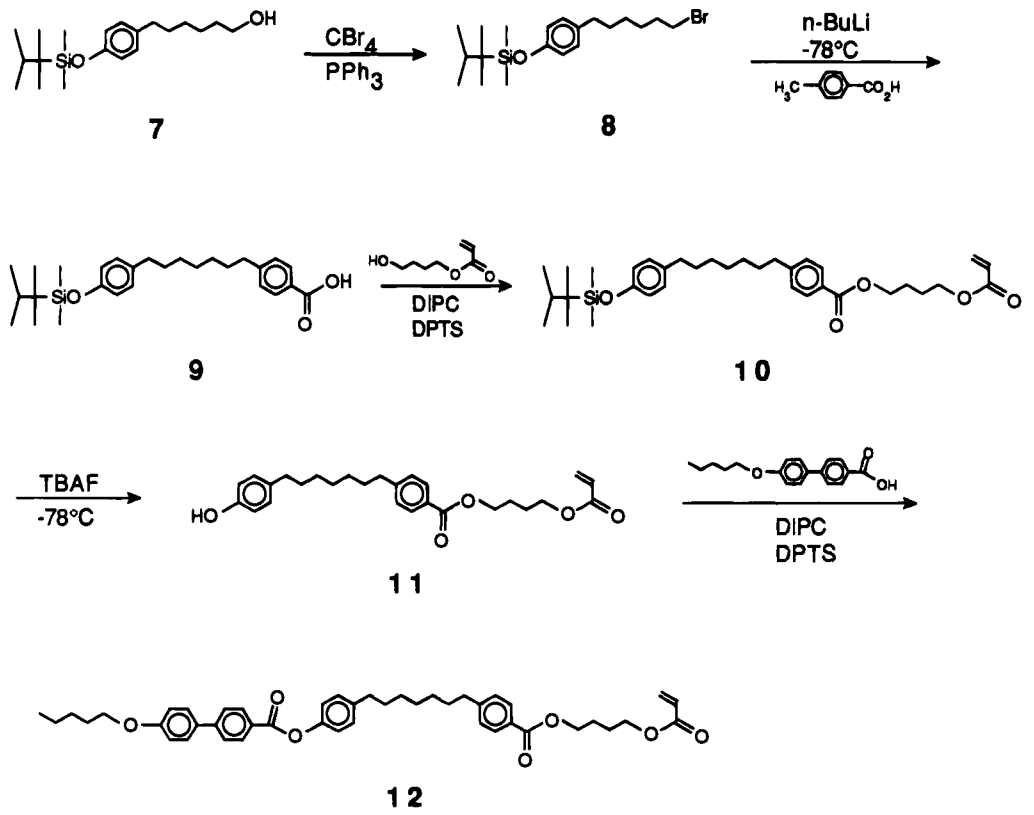

which should bring nitrile groups closer to each other. One important unknown at the moment is the mechanism of initiation for this reaction in the ordered assembly. On the basis of previous work,[30] one reasonable possibility would be migration of the tertiary hydrogen resulting in the cationic initiation of the reaction by methylenimino groups. This possibility is described in Scheme 4. A new peak possibly corresponding to N−H bonds was observed in the infrared spectrum after the

(29) Kubasova, N. A.; Dinh-Suang-Dihn-Dihn; Geiderikh, M. A.; Shishkina, M. V. *Vysokomol. Soedin., Ser. A* **1971**, *13*, 162. Geiderikh, M. A.; Dinh-Suang-Dihn-Dihn; Davydov, B. E.; Karpacheva, G. P. *Vysokomol. Soedin., Ser. A* **1973**, *15*, 1239.

(30) Davydov, B. E.; Krentsel, B. A. *Advances in Polymer Science*; Springer-Verlag: Berlin, Heidelberg, New York, 1977; Vol. 25, p 12.

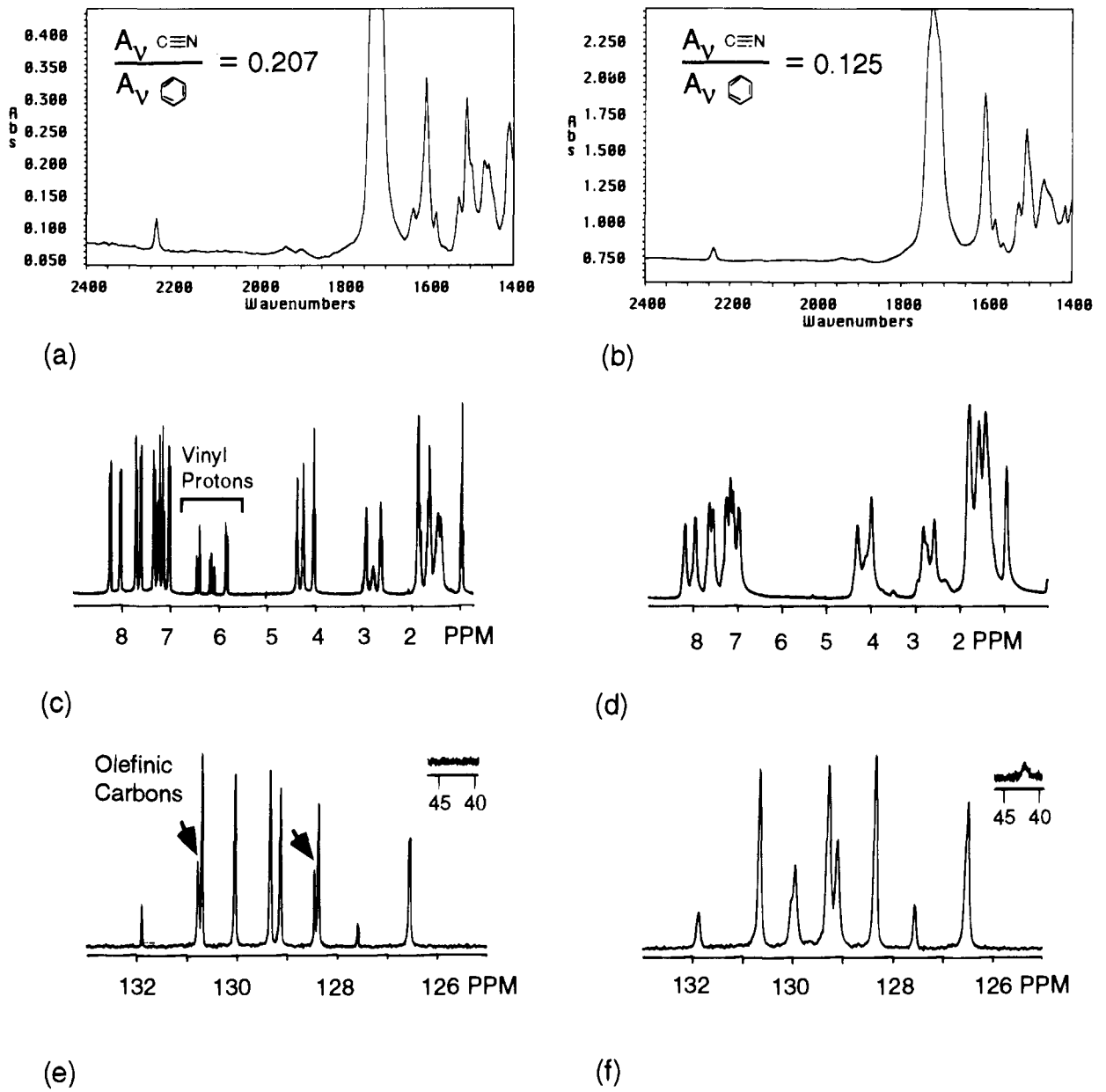

Figure 11. Infrared and NMR spectra of **6** and its corresponding 2D polymer product. Infrared spectra of **6** (a) and 2D polymer (b); ^{1}H NMR (c and e) and ^{13}C NMR (d and f) of **6** and 2D polymer, respectively.

Scheme 3

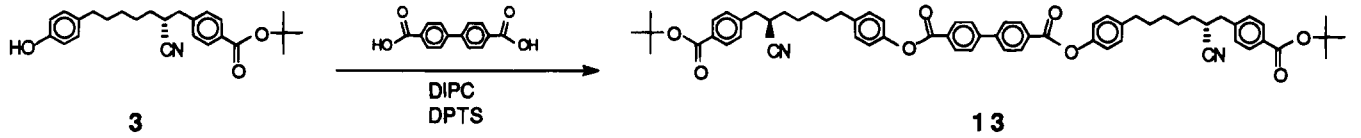

Scheme 4

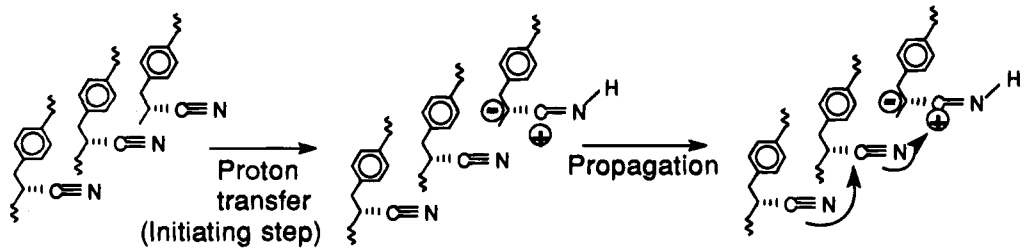

reaction near 3400 cm^{-1}. Because of steric constraints revealed to us by molecular models, we expect the oligoimine sequences to be fairly short, perhaps in the trimeric to pentameric range.

Relative to poly(styrene) standards, gel permeation chromatography (GPC) of THF solutions indicates the molar mass of the 2D polymers obtained could be as high as 17 000 000 Da. This is inferred on the basis of extrapolation of elution time vs molecular weight curves obtained using poly(styrene) standards

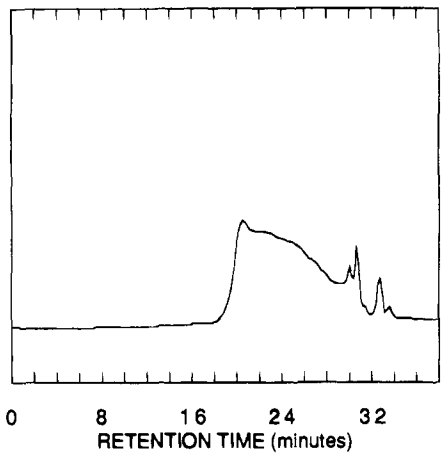

Figure 12. Gel permeation chromatograph of the 2D polymer product obtained from **6**.

(the highest molecular weight standard used had a molar mass of 3 100 000 Da). Figure 12 shows a typical GPC curve of the product after a 10% by weight insoluble fraction was removed. The curve reveals a non-Gaussian chromatogram with the largest weight fraction in the product corresponding to a molar mass of 2 700 000, a weight average molecular weight of 880 000, and a polydisperity value of 56. It is possible that adhesion of macromolecules to the GPC column takes place, thus complicating the interpretation of the chromatogram. Poly(styrene) standards and currently used packing materials are of questionable value in the characterization of this type of product. This is suggested given the drastic differences expected in hydrodynamic shape between 2D polymers and coils formed by flexible linear chains. New techniques may have to be developed in order to characterize the molar mass of molecular object polymers with nonglobular shape.

As the temperature rises, the smectogenic nature of the precursor should stabilize the shape of planar objects. This is suggested because at the local concentration of precursor units prevailing in the interior of 2D polymer molecules, layered structures could be thermodynamically stable within a given temperature range. The factors preventing the collapse of the object are both the molecular rigidity of monomer units and the fact that covalent backbones stitching the interior prevent a significant decrease of the local monomer concentration within the object. In a solution of these 2D polymers, one way to view the object's stability is to consider that covalent bonds among monomers maintain local concentrations above the critical point of an Onsager transition of rods from disordered to ordered states. The factors responsible for thermodynamic stability of liquid crystalline smectic phases formed by the precursors might also suppress shape deformations in the planar object.

Computer Simulation. We used a computer simulation to evaluate what extents of reaction and average degrees of polymerization may be necessary to form large 2D objects. The model system for the simulation was a bilayered lattice of rods representing precursor molecules. There were therefore three planes of reactive sites in the lattice, the middle one containing the acrylate groups and the two outer ones containing the nitriles. We refer to the middle plane as the "main" plane and the other two as the "satellite" planes. As the degree of polymerization (DP) is increased in each layer, larger and fewer objects should form. A schematic representation of the system used in the simulation is shown in Figure 13. Based on spectroscopic data, the simulation assumes that 30% of the nitriles and 90% of the acrylate groups react. The simulation also assumes that acrylates[31] oligomerize to a DP of 10 and nitriles to DP values between 2 and 5.[32]

The algorithm was tested on different lattices containing between 10 000 and 1 000 000 sites (each representing two precursor molecules of the bilayer).[33] Planar random walks to connect the sites were run in each of the three planes of the lattice, and all walks were initiated simultaneously. The simulation with 25 000 sites in the lattice made, for example, 22 500 walks in the main plane with a DP of 10 and 37 500 walks in satellite planes when a DP of 2 was used.[34] The choice of a square lattice was arbitrary and not intended to reflect the nature of molecular packing in the layered assemblies. After the walks reached the targeted extents of reaction, the lattice was separated into its component objects containing one or more sites joined by connections in any of the three planes. Each run therefore generates a population of objects containing different numbers of precursors.

The results of the simulations indicate that only a small number of precursor molecules of the lattice needs to be connected by a given stitching backbone in order to form large 2D molecular objects. This is clear from inspection of Figure 14 which plots as a function of satellite plane DP the fraction of precusor molecules in the lattice that become part of the largest object formed. It is interesting that only pentamerization of precursors in the satellite planes is necessary to create an object containing approximately 700 000 precursor molecules in the 1 000 000-site lattice. This object would have an aspect ratio of 100:1 based on the measured thickness of 2D polymers imaged by electron microscopy. The percent of precursors catenated into the largest object is apparently independent of lattice size, on the basis of other simulations with smaller lattices. A different representation of the data is shown in Figure 15 which plots the number of objects formed as a function of satellite DP, and as expected the number of objects decreases with increasing DP. Another simulation which only considers overall extents of reaction and not specific layer DPs was carried out by Munkel and Heermann[35] shortly after our original description of the experimental system.[13] On the basis of the simulation and results from percolation theory, the authors conclude that our reported extents of reaction are high enough to produce an "infinite" 2D polymer.

The computer simulations illustrate the importance of molecular recognition events among similar molecular segments of precursor molecules, most importantly among the reactive functions. The precursor molecules of interest here lack a center of inversion; thus we must consider the sense of their orientation within the layer. The simulations described above assume that all precursor molecules in the layered assembly have the same orientation, and therefore the functional groups are confined to planes (see Figure 16a). However, in order to explore the importance of molecular recognition, we considered if reactions within layers of randomly oriented precursors could lead to large objects. The illustration in Figure 16b shows a schematic representation of layers of precursor molecules with random orientation and a cross section of the resultant macromolecules after reaction. It is clear that neighboring precursor molecules

(31) The choice of DP = 10 was based on the average degree of polymerization obtained when precursor **6** is polymerized in dilute solution using free radical initiation.

(32) Following examination of molecular models, we selected low degrees of catenation among nitriles on the basis of the possibility of steric problems as the stitching reactions proceed.

(33) The program for the simulation was first written in C on a Compaq 386/25 workstation. It was then ported to an RS6000 workstation and subsequently to an Indigo Elan workstation.

(34) It is not possible to predict in advance how many random walks will dead end when the program is run. Therefore it is difficult to obtain exactly the correct bond density and average DP in a layer. Typically final values fell within 1% of the targeted values. If desired, the code could be altered to correct this premature chain termination, by allowing walks which do not dead end to continue well past the desired DP.

(35) Munkel, C.; Heerman, D. W. *Physica A* **1993**, *199*, 12.

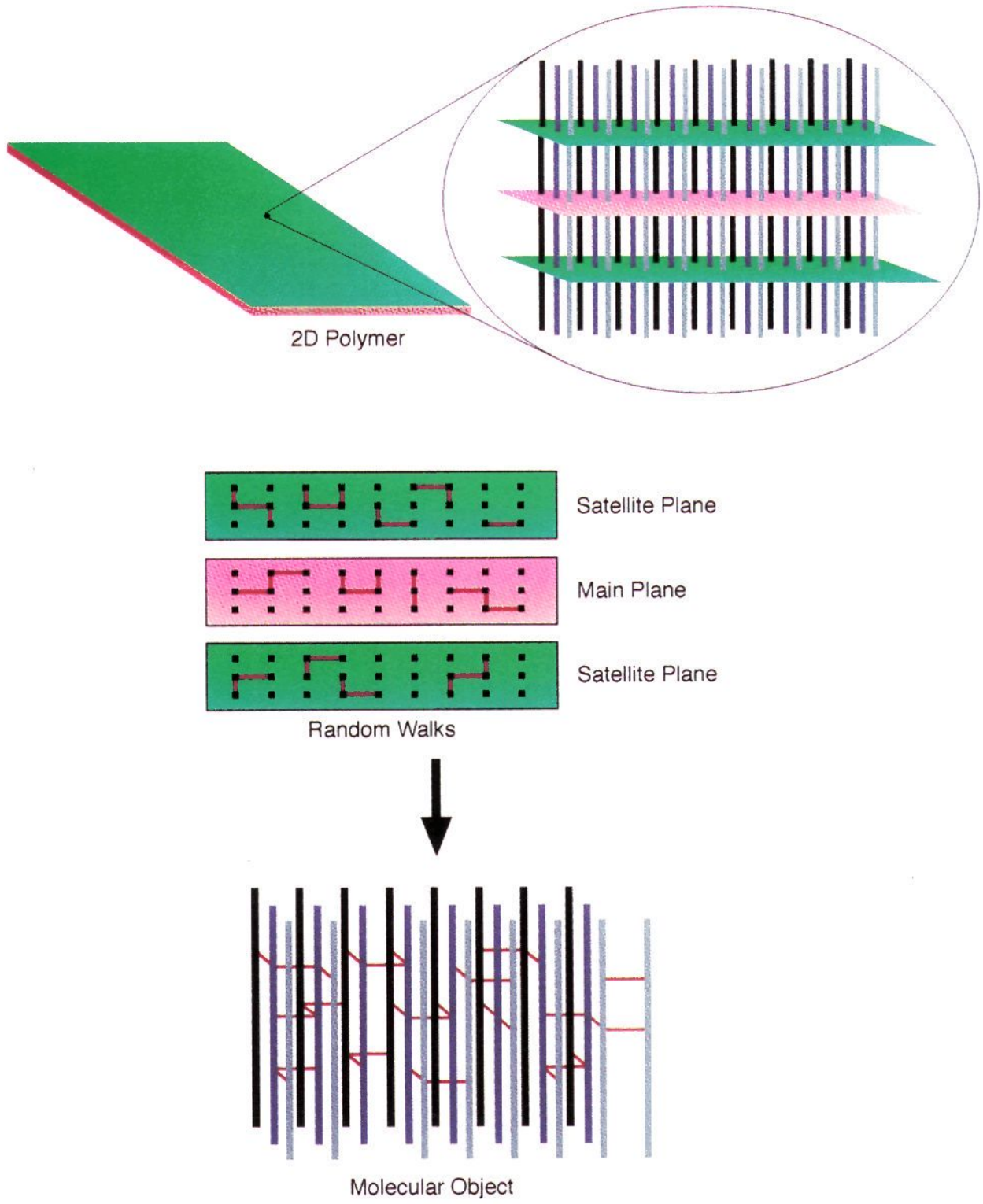

Figure 13. Schematic representation of the computer simulation of 2D polymer growth.

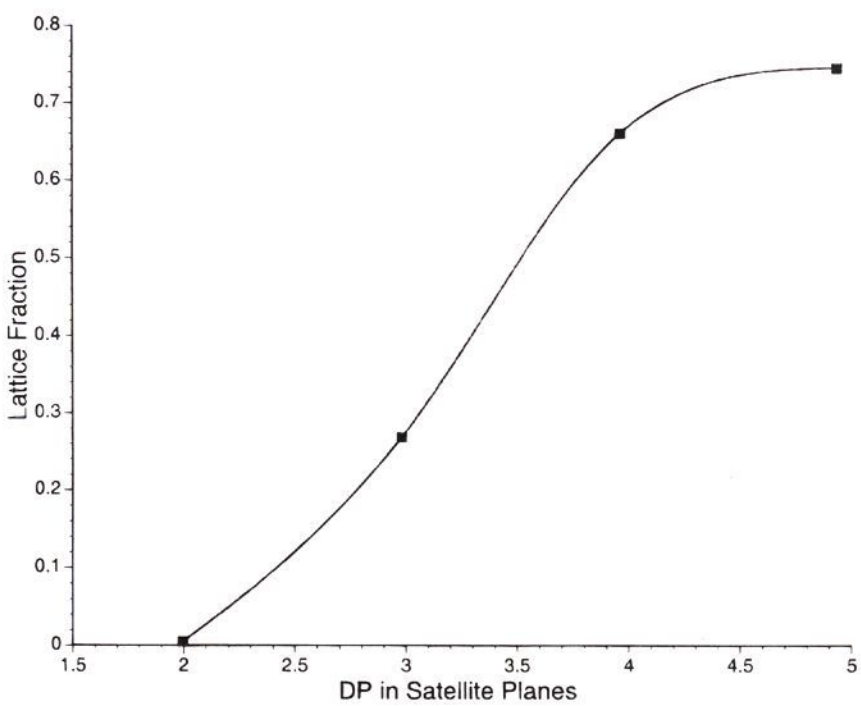

Figure 14. Fraction of precursor molecules in a lattice containing 1 000 000 sites which are connected by random walks as a function of the degree of polymerization in satellite planes (see text).

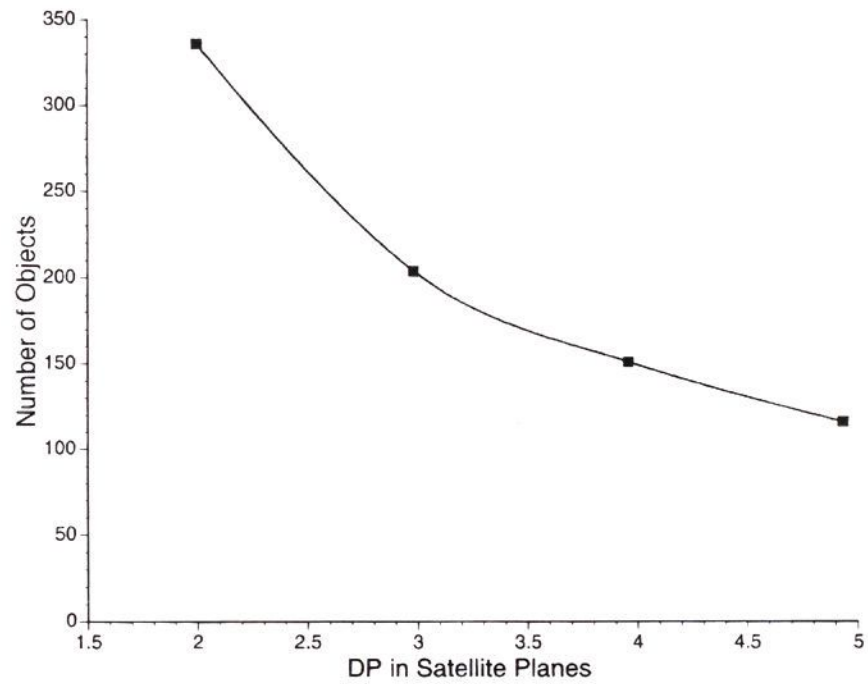

Figure 15. Number of molecular objects formed by the random walks in a lattice containing 1 000 000 sites as a function of the degree of polymerization in satellite planes (see text).

in two contiguous layers with the proper orientation to react in all three planes defined before cannot connect covalently to molecules in neighboring layers. Those neighboring molecules of the two contiguous layers which are not in the correct orientation to react in all three planes can only connect to molecules in neigboring layers. The end result is the formation of macromolecules with rough surfaces which can be separated from each other as shown in the schematic representation. Once disassembled from the layers, by solvation for example, these

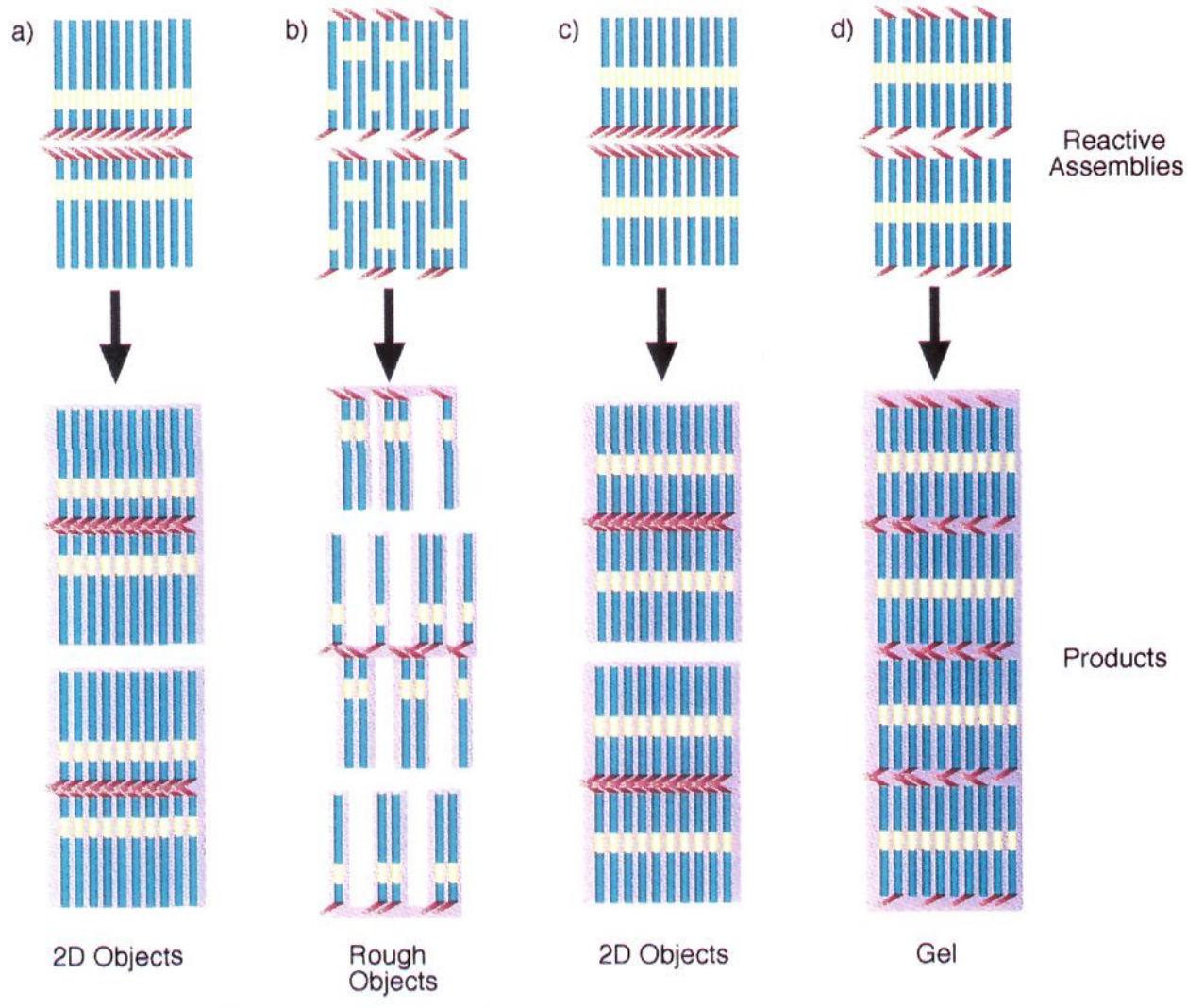

Figure 16. Schematic representation of the nature of products formed after reactions in various types of layered molecular assemblies (features on the rods represent reactive functions). (a) Finite 2D polymers form after reaction in a bilayer which is orientationally ordered by molecular recognition events (precursor molecules in this case are analogous to those in **6**). (b) Molecular objects with very rough surface form in orientationally disordered layers. (c) Finite 2D objects form as in panel a from precursors containing a reactive function at the center of their molecular backbone. (d) An infinite network gel forms from the orientationally disordered version of bilayer c.

macromolecules could not be easily restacked into dense layers as a result of mismatch in their surface landscapes. Furthermore, these macromolecules are not likely to a have persistent 2D shape given the sparsity of rodlike precursors in each bilayer. In a solvent the rough-surfaced macromolecules would likely collapse or crumple into various shapes which are not necessarily two-dimensional.

The molecular arrangement shown in Figure 16b is likely to occur when molecular recognition is not a predominant feature of the system. If one of the reactive functions were to be placed in the center of precursor molecules and molecules were arranged with common orientation (Figure 16c), 2D polymers would form. However, random orientation in this system (Figure 16d) would lead to gelation into an infinite network. In fact, this same gelation would also occur if one were to allow the off-center functions of layers shown in Figure 16b to react. Complete gelation was never observed in our experimental system, and thus in order to explore the effect of molecular recognition events, we carried out a simulation in which off-center functions were not able to react in layers with randomly oriented precursor molecules. In this configuration only neighboring precursors pointing in the same direction could react to stitch the molecular object. Since the reactive assembly is a bilayer of precursor molecules, the simulation was done introducing 50% vacant sites in satellite planes but only 25% vacant sites in the main plane. This is of course because precursor molecules with opposite orientation in two contiguous layers could still contribute reactive functional groups to the middle plane. The results of this simulation are very interesting and are shown in Figure 17. This figure compares plots of fraction of precursors in the largest object formed as a function of satellite DP for layers in which molecular recognition prevails (Figure 16a) vs layers with random orientation of precursor molecules (Figure 16b). The simulation using a 1 000 000-site

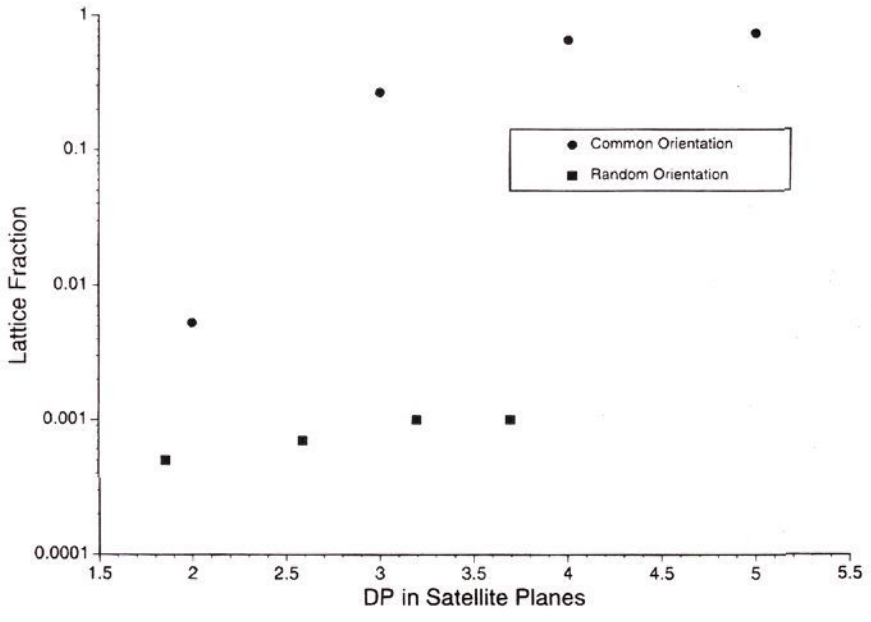

Figure 17. Plots in a logarithmic scale of the fraction of precursor molecules connected by random walks when the bilayer assembly is orientationally ordered (●) and when layers contain randomly oriented precursor molecules (■).

lattice shows that large 2D molecular objects do not form when the arrangement of precursor molecules is random, and thus molecular recognition events do not control molecular orientation within the layers.

Conclusions

The bulk synthesis of a shape persistent 2D polymer of high molar mass can be accomplished with rigid precursor molecules that self-assemble into bilayers with internal orientational order. The orientational order of molecules within the bilayers confines reactive functions to planes and facilitates covalent stitching of precursors into flat polymers. Stereocenters that participate in molecular recognition events can effectively encode in the

precursor's structure the formation of the orientationally ordered planar assemblies required for the synthesis. "Bulk" syntheses of shape persistent 2D polymers which do not require external boundaries to confine monomers into 2D spaces may lead to many interesting advanced materials.

Experimental Section

Precursor Synthesis. *tert*-Butyl 4-[(2*R*)-2-Cyano-7-[(4[(dimethylthexylsilyl)oxy]phenyl]heptylidene]benzoate (2). To a stirred suspension of **1** (14.6 g, 22.4 mmol) and SeO_2 (2.0 g, 18 mmol) in 227 mL of methanol was added 30% H_2O_2 (7.3 mL) at once. After being stirred at room temperature for 30 min, the solution was transferred to a separatory funnel containing 700 mL of CH_2Cl_2. The combined organic layer was washed with brine water (600 mL), dried ($MgSO_4$), and then concentrated. The residue was purified by flash chromatography using a mixture of petroleum ether−EtOAc (9:1) as eluent to give 10.7 g (89% yield) of **2** as an oil: MS (FAB) 535 (M^+); ^{1}H NMR (300 MHz, $CDCl_3$, TMS) δ 0.20 (s, 6H), 0.93 (s, 6H), 0.93 (d, J = 6.8 Hz, 6 H) 1.3−1.7 (m, 17H), 1.58 (s, 9H), 2.51 (t, J = 7.4 Hz, 2H), 2.7−2.8 (m, 1H), 2.90−2.94 (m, 2H), 6.73 (d, J = 8.3 Hz, 2H), 6.99 (d, J = 8.3 Hz, 2H), 7.26 (d, J = 8.1 Hz, 2H), 7.95 (d, J = 8.1 Hz, 2H);^{13} C NMR (75 MHz, $CDCl_3$) δ −2.41 (CH_3), 18.63 (CH_3), 20.21 (CH_3), 25.01 (C), 26.99 (CH_2), 28.20 (CH_3), 28.55 (CH_2), 31.28 (CH_2), 31.74 (CH_2), 33.51 (CH), 34.17 (CH), 34.90 (CH_2), 38.26 (CH_2), 80.97 (C), 119.89 (CH), 121.42 (C), 128.91 (CH), 129.18 (CH), 129.88 (CH), 131.06 (C), 134.90 (C), 141.70 (C), 153.43 (C), 165.40 (C). Anal. Calcd for $C_{37}H_{45}NO_3Si$ (535.83): C, 73.65; H, 9.08; N, 2.68. Found: C, 73.66; H, 9.15; N, 2.67.

***tert*-Butyl 4-[(2*R*)-2-Cyano-7-(4-hydroxyphenyl)heptylidene]benzoate (3).** A solution of **2** (2.2 g, 4.1 mmol) in dry THF (17 mL) was stirred at room temperature for 5 min to form a homogeneous solution and then cooled to −78 °C under nitrogen. With vigorous stirring, TBAF (6.1 mL of a 1.0 N solution in THF) was added dropwise via cannula. After the mixture was stirred for 2 h at −78 °C, 1.5 mL of TBAF solution was further added and stirring was continued for an additional 1 h. At this point, the reaction was quenched with a solution of acetic acid (340 mg) in diethyl ether (34 mL) at −78 °C. The contents were poured into 300 mL of H_2O and extracted with ether (2 × 150 mL) followed by washing with brine water (150 mL). The organic layer was dried ($MgSO_4$) and concentrated. This compound was pure enough to be used for the next step (quantitative yield): ^{1}H NMR (300 MHz, $CDCl_3$, TMS) δ 1.31−1.86 (m, 8H), 1.59 (s, 9H), 2.53 (t, J = 7.7 Hz, 2H), 2.55 (m, 1H), 2.90−2.95 (m, 2H), 6.76 (d, J = 8.3 Hz, 2H), 7.03 (d, J = 8.4 Hz, 2H), 7.28 (d, J = 8.3 Hz, 2H), 7.97 (d, J = 8.2 Hz, 2H).

***tert*-Butyl 4-[(2*R*)-2-Cyano-7-[(4[[[4′-(pentyloxy)-4-biphenyl]carbonyl]oxy]phenyl]heptylidene]benzoate (4).** To a suspension of **3** (1.6 g, 4.1 mmol), 4-pentoxybiphenylcarboxylic acid (1.15 g, 3.9 mmol), and DPTS (603 mg, 2.2 mmol) in dry CH_2Cl_2 (62 mL) was added 1.07 mL of DIPC (6.8 mmol) at room temperature under nitrogen. The mixture was stirred for 36 h at room temperature, and the solid precipitate (urea) was removed by vacuum filtration followed by evaporation of the solvent. The residue was purified by flash chromatography using a mixture of 2% EtOAC in CH_2Cl_2 as eluent to give 2.16 g (80% yield) of **4** as a solid: mp 84 °C; MS (FAB) 660 (M^+); ^{1}H NMR (300 MHz, $CDCl_3$, TMS) δ 0.93−0.97 (m, 3H), 1.38−1.75 (m, 14H), 1.59 (s, 9H), 2.63 (t, 2H), 2.78 (m, 1H), 2.94 (t, 2H), 4.04 (t, J = 6.5 Hz, 2H), 7.02 (d, J = 8.7 Hz, 2H), 7.15 (d, J = 8.5 Hz, 2H), 7.24 (d, J = 8.7 Hz, 2H), 7.31 (d, J = 8.3 Hz, 2H), 7.62 (d, J = 8.7 Hz, 2H), 7.71 (d, J = 8.4 Hz, 2H), 7.98 (d, J = 8.2 Hz, 2H), 8.25 (d, J = 8.4 Hz, 2H); ^{13}C NMR (75 MHz, $CDCl_3$), δ 14.07 (CH_3), 22.49 (CH_2), 27.00 (CH_2), 28.20 (CH_3), 28.56 (CH_2), 28.96 (CH_2), 31.07 (CH_2), 31.74 (CH_2), 33.55 (CH_2), 35.13 (CH_2), 38.30 (CH_2), 68.14 (CH_2), 81.06 (C), 114.97 (CH), 121.44 (C), 121.49 (CH), 126.57 (CH), 127.57 (C), 128.38 (CH), 128.90 (CH), 129.33 (CH), 129.90 (CH), 130.69 (CH), 131.08 (C), 131.97 (C), 139.87 (C), 141.61 (C), 145.91 (C), 149.01 (C), 159.56 (C), 165.31 (C), 165.46 (C). Anal. Calcd for $C_{43}H_{49}O_5N$ (660.4): C, 78.27; H, 7.49; N, 2.12. Found: C, 78.26; H, 7.52; N, 2.15.

4-[(2*R*)-2-Cyano-7-[4-[[[4′-(pentyloxy)-4-biphenyl]carbonyl]oxy]-phenyl]heptylidene]benzoic Acid (5). To a solution of **4** (2.1 g, 3.2 mmol) in dry CH_2Cl_2 (10 mL) was added 3.3 mL of CF_3CO_2H at room temperature under nitrogen. The solution was stirred for 4.5 h, and then solvent and TFA were removed by rotary evaporation and high vacuum. The remaining solid was dissolved in a minimum amount of CH_2Cl_2 followed by addition of pentane until the permanent cloudiness formed. The precipitate was collected by vacuum filtration and dried in a vacuum dessicator to give 1.5 g (79% yield) of product **5**: mp 180 °C; ^{1}H NMR (300 MHz, $CDCl_3$, TMS) δ 0.95 (t, J = 6.9 Hz, 3H), 1.37−1.85 (m, 14H), 2.64 (t, J = 7.5 Hz, 2H), 2.66 (m, 1H), 2.76 (t, J = 5.2 Hz, 2H), 4.02 (t, J = 6.6 Hz, 2H), 7.02 (d, J = 8.6 Hz, 2H), 7.15 (d, J = 8.4 Hz, 2H), 7.26 (d, J = 8.1 Hz, 2H), 7.36 (d, J = 8.1 Hz, 2H), 7.61 (d, J = 8.1 Hz, 2H), 7.69 (d, J = 8.2 Hz, 2H), 8.10 (d, J = 8.0 Hz, 2H), 8.24 (d, J = 8.2 Hz, 2H); ^{13}C NMR (75 MHz, $CDCl_3$) δ 14.07 (CH_3), 22.50 (CH_2), 26.96 (CH_2), 28.22 (CH_2), 28.50 (CH_2), 28.96 (CH_2), 31.03 (CH_2), 31.87 (CH_2), 33.43 (CH), 35.12 (CH_2), 38.39 (CH_2), 68.15 (CH_2), 114.98 (CH), 121.34 (C), 121.51 (CH), 125.72 (C), 126.57 (CH), 127.55 (C), 128.39 (CH), 129.23 (CH), 129.34 (CH), 130.71 (CH), 131.96 (C), 139.86 (C), 143.22 (C), 145.91 (C), 149.02 (C), 159.56 (C), 165.35 (C), 171.68 (C). Anal. Calcd for $C_{39}H_{41}O_5N$ (603.8): C, 77.58; H, 6.85; N, 2.31. Found: C, 77.39; H, 6.95; N, 2.37.

(Acrylyloxy)-1,4-tetramethylene-4-[(2*R*)-2-Cyano-7-[4-[[[4′-(pentyloxy)-4-biphenyl]carbonyl]oxy]phenyl]heptylidene]benzoate (6). To a suspension of **5** (1.2 g, 1.99 mmol), DPTS (360 mg, 1.22 mmol), and 4-hydroxybutyl acrylate (0.92 mL, 6.64 mmol) in dichloromethane (18 mL), at room temperature, was added DIPC (0.6 mL, 3.8 mmol) with vigorous stirring under nitrogen. After being stirred for 24 h, the solid precipitate (urea) was removed by suction filtration followed by evaporation of the solvent. The product was purified by flash chromatography on silica gel using a mixture of 2% acetone in dichloromethane to give 1.14 g (78.5% yield) of product **6** as a white solid: MS (FAB) 730 (M^+); ^{1}H NMR (300 MHz, $CDCl_3$, TMS) δ 0.94 (t, J = 6.8 Hz, 3H), 1.38−1.85 (m, 18H), 2.62 (t, J = 7.4 Hz, 2H), 2.65 (m, 1H), 2.76−2.95 (m, 2H), 4.00 (t, J = 6.5 Hz, 2H), 4.23 (t, J = 5.0 Hz, 2H), 4.35 (t, J = 5.5 Hz, 2H), 5.80−6.40 (m, 3H), 7.01 (d, J = 8.4 Hz, 2H), 7.14 (d, J = 8.4 Hz, 2H), 7.22 (d, J = 8.3 Hz, 2H), 7.33 (d, J = 8.1 Hz, 2H), 7.60 (d, J = 8.4 Hz, 2H), 7.69 (d, J = 8.2 Hz, 2H), 8.03 (d, J = 8.0 Hz, 2H), 8.23 (d, J = 8.1 Hz, 2H); ^{13}C NMR (75 MHz, $CDCl_3$) δ 14.08 (CH_3), 22.49 (CH_2), 25.43 (CH_2), 25.47 (CH_2), 26.98 (CH_2), 28.22 (CH_2), 28.55 (CH_2), 28.97 (CH_2), 31.05 (CH_2), 31.79 (CH_2), 33.48 (CH), 35.12 (CH_2), 38.30 (CH_2), 64.03 (CH_2), 64.46 (CH_2), 68.12 (CH_2), 115.00 (CH), 121.37 (C), 121.50 (CH), 126.53 (CH), 127.57 (C), 128.36 (CH), 128.43 (CH), 129.12 (CH), 129.32 (CH), 130.02 (CH), 130.69 (CH), 130.76 (CH_2), 131.88 (C), 139.85 (C), 142.31 (C), 145.87 (C), 149.06 (C), 159.60 (C), 165.24 (C), 166.20 (C). Anal. Calcd for $C_{46}H_{51}O_7N$ (729.88): C, 75.69; H, 7.04; N, 1.92. Found: C, 75.61; H, 6.99; N, 1.93.

1-Bromo-6-[4-[(dimethylexylsilyl)oxy]phenyl]hexane (8). In a 25 mL round-bottomed three-neck flask, equipped with a thermometer, nitrogen inlet, and rubber septum, **7** (1.62 g, 4.81 mmol) was dissolved in CH_3CN (1.7 mL). A solution of CBr_4 (1.94 g, 5.8 mmol) in CH_3CN (4.7 mL) was added to the above solution through a cannula with vigorous stirring. Remaining CBr_4 solution was washed with CH_3CN (0.8 mL) and added to the reaction mixture. In one portion, 1.54 g of PPh_3 (5.8 mmol) was then added to the reaction mixture placed in a room temperature water bath. After being stirred for 2 h, the solvent was removed by rotary evaporation followed by high vacuum. The residue was added to a 2:1 ratio of diethyl ether and pentane to give the precipitate. The precipitate was removed by vacuum filtration followed by concentration of the solution by rotary evaporoation. The residue was purified by flash chromatography with 1% Et_2O in petroleum ether to give 1.6 g (83.3% yield) of **8** as a syrup: MS (FAB) 400 (M^+); ^{1}H NMR (300 MHz, $CDCl_3$, TMS) δ 0.23 (s, 6H), 0.96 (d, J = 6.8 Hz, 6H), 1.35−1.89 (m, 9H), 2.55 (t, J = 7.8 Hz, 2H), 3.41 (t, J = 13.7 Hz, 2H), 6.75 (d, J = 8.3 Hz, 2H), 7.03 (d, J = 8.3 Hz, 2H); ^{13}C NMR (75 MHz, $CDCl_3$) δ −2.47 (CH_3), 18.56 (CH_3), 20.15 (CH_3), 24.97 (C), 28.00 (CH_2), 28.28 (CH_2), 31.39 (CH_2), 32.72 (CH_2), 33.93 (CH_2), 34.12 (CH), 34.94 (CH_2), 119.80 (CH), 129.10 (CH), 135.07 (C), 153.34 (C). Anal. Calcd for $C_{20}H_{35}BrOSi$ (399.48): C, 60.13; H, 8.83; Br, 20.00. Found: C, 60.03; H, 8.22; Br, 20.28.

4-[7-[4-[(Dimethylthexylsilyl)oxy]phenyl]heptylidene]benzoic Acid (9). A dry 50 mL, three-neck flask connected to a nitrogen inlet and two rubber septums was charged with potassium *tert*-butoxide (0.91 g, 8.11 mmol), and the flask was flushed with argon gas. Dry THF (9

mL) was added via cannula, and the suspension was cooled to −78 °C. Diisopropylamine (1.1 mL, 8.05 mmol) was then added followed by dropwise addition of a 1.6 N *n*-butyllithium solution in hexane (4.84 mL, 7.73 mmol) over a 10 min period. After stirring an additional 15 min, a solution of *p*-toluic acid (0.5 g, 3.67 mmol) in THF (3 mL) was slowly added via cannula. Stirring at −78 °C was continued for 4 h. At this point, a solution of **8** (1.47 g, 3.68 mmol) in THF (2.5 mL) was added. After the mixture was stirred for 30 min, the temperature was allowed to rise slowly to 0 °C over a 2 h period, and the mixture was transferred to a separatory funnel containing diethyl ether (80 mL) and 1 N HCl (150 mL). The organic layer was collected after vigorous shaking, dried ($MgSO_4$), and concentrated in vacuo. The concentrated reaction mixture was purified by flash chromatography with 3% MeOH in $CHCl_3$ to give 750 mg (45% yield) of product as solid **9**: MS (FAB) 455 (M^+); ^{1}H NMR (300 MHz, $CDCl_3$, TMS) δ 0.23 (s, 6H), 0.96 (s, 6H), 1.35−1.65 (m, 11H), 2.54 (t, J = 7.8 Hz, 2H), 2.68 (t, J = 7.3 Hz, 2H), 6.75 (d, J = 8.4 Hz, 2H), 7.04 (d, J = 8.4 Hz, 2H), 7.29 (d, J = 8.3 Hz, 2H), 8.05 (d, J = 8.2 Hz, 2H); ^{13}C NMR (75 MHz, $CDCl_3$) δ −2.43 (CH_3), 18.60 (CH_3), 20.19 (CH_3), 25.01 (C), 29.14 (CH_2), 29.19 (CH_2), 29.32 (CH_2), 31.09 (CH_2), 31.64 (CH_2), 34.17 (CH), 35.11 (CH_2), 36.11 (CH_2), 119.81 (CH), 126.79 (C), 128.58 (CH), 129.15 (CH), 130.31 (CH), 135.39 (C), 149.56 (C), 153.31 (C), 172.50 (C). Anal. Calcd for $C_{28}H_{42}O_3Si$ (454.71): C, 73.96; H, 9.31. Found: C, 73.92; H, 9.37.

(Acrylyloxy)-1,4-tetramethylene-4-[7-[4-[(Dimethylthexylsilyl)-oxy]phenyl]heptylidene]benzoate (10). In a dry 50 mL, single-neck flask, **9** (550 mg, 1.12 mmol) and DPTS (208 mg, 0.71 mmol) were suspended in CH_2Cl_2 (10 mL), under nitrogen atmosphere. Then 4-hydroxybutyl acrylate (0.52 mL, 3.75 mmol) was added at once followed by the addition of DIPC (0.32 mL, 2.04 mmol). After being stirred for 25 h, the solid precipitate was removed by vacuum filtration followed by evaporation of the solvent. The concentrated reaction mixture was purified by flash chromatography using $CHCl_3$ as eluent to give 620 mg (88.2% yield) of **10** as a syrup: MS (FAB) 581 (M^+); ^{1}H NMR (300 MHz, $CDCl_3$, TMS) δ 0.21 (s, 6H), 0.94 (s, 6H), 0.94 (d, J = 6.8 Hz, 6H), 1.32−1.87 (m, 15H), 2.51 (t, J = 7.9 Hz, 2H), 2.65 (t, J = 7.9 Hz, 2H), 4.24 (t, J = 5.6 Hz, 2H), 4.35 (t, J = 5.6 Hz, 2H), 5.83 (dd, J = 0.8, 10.4 Hz, 1H), 6.10 (q, J = 10.3, 17.3 Hz, 1H), 6.41 (d, J = 17.4 Hz, 1H), 6.73 (d, J = 8.3 Hz, 2H), 7.01 (d, J = 8.3 Hz, 2H), 7.23 (d, J = 8.1 Hz, 2H), 7.95 (d, J = 8.2 Hz, 2H); ^{13}C NMR (75 MHz, $CDCl_3$) δ −2.45 (CH_3), 18.58 (CH_3), 20.17 (CH_3), 24.99 (C), 25.44 (CH_2), 25.49 (CH_2), 29.14 (CH_2), 29.17 (CH_2), 29.32 (CH_2), 31.14 (CH_2), 31.63 (CH_2), 34.14 (CH_2), 35.10 (CH_2), 36.00 (CH_2), 64.08 (CH_2), 64.22 (CH_2), 119.79 (CH), 127.69 (CH), 128.44 (CH), 129.13 (CH), 129.60 (C), 130.77 (CH_2), 135.38 (C), 148.52 (C), 153.30 (C), 166.22 (C), 166.65 (C). Anal. Calcd for $C_{35}H_{52}O_5Si$ (580.86): C, 72.37; H, 9.02. Found: C, 72.25; H, 9.04.

(Acrylyloxy)-1,4-tetramethylene 4-[7-(4-Hydroxyphenyl)heptylidene]benzoate (11). A dry, 25 mL single-neck flask fitted with a Claisen adapter connected to a nitrogen inlet and a rubber septum was charged with **10** (550 mg, 0.95 mmol) and dry THF (4 mL). The solution was stirred at room temperature to form a homogeneous solution and then cooled to −78 °C. To the solution was added TBAF (1 N in THF, 1.83 mL) via cannula. After the mixture was stirred for 80 min, the reaction was quenched with a solution of acetic acid (80 mg) in ether (8 mL) at −78 °C. The solution was transferred to a separatory funnel containing 80 mL of diethyl ether and 80 mL of water. After being shaken vigorously, the organic layer was collected and then washed with saturated $NaHCO_3$ and brine. After drying over $MgSO_4$, the solvents were removed under reduced pressure. The crude product was used for the next step without further purification.

(Acrylyloxy)-1,4-tetramethylene 4-[7-[4-[[[4′-(Pentyloxy)-4-biphenyl]carbonyl]oxy]phenyl]heptylidene]benzoate (12). In a dry, 50 mL single-neck flask connected to a nitrogen inlet, **11** (417 mg, 0.95 mmol), 4-hydroxybiphenylcarboxylic acid (270 mg, 0.95 mmol), and DPTS (141 mg, 0.48 mmol) were suspended in dry CH_2Cl_2 (14 mL). To the suspension was added DIPC (0.22 mL, 1.41 mmol). After being stirred for 18 h, the solid precipitate was removed by vacuum filteration followed by evaporation of the solvent. The concentrated mixture was purified by flash chromatography with a mixture of 50% CH_2Cl_2 in $CHCl_3$ as eluent to give 580 mg (86.6% yield) of **12**: MS (FAB) 705 (M^+); ^{1}H NMR (300 MHz, $CDCl_3$, TMS) δ 0.95 (t, J = 7.0 Hz, 3H), 1.35−1.87 (m, 23H), 2.60−2.69 (m, 4H), 4.02 (t, J = 6.6 Hz, 2H), 4.24 (t, J = 5.9 Hz, 2H), 4.35 (t, J = 5.7 Hz, 2H), 5.83 (dd, J = 1.14, 10.3 Hz, 1H), 6.13 (q, J = 8.7, 10.37 Hz, 1H), 6.41 (d, J = 17.1 Hz, 1H), 7.01 (d, J = 8.6 Hz, 2H), 7.13 (d, J = 8.4 Hz, 2H), 7.00−7.30 (m, 4H), 7.60 (d, J = 8.6 Hz, 2H), 7.69 (d, J = 8.4 Hz, 2H), 7.96 (d, J = 8.1 Hz, 2H), 8.23 (d, J = 8.3 Hz, 2H); ^{13}C NMR (75 MHz, $CDCl_3$) δ 14.06 (CH_3), 22.49 (CH_2), 25.45 (CH_2), 28.21 (CH_2), 28.96 (CH_2), 29.15 (CH_2), 29.32 (CH_2), 31.13 (CH_2), 31.43 (CH_2), 35.36 (CH_2), 36.00 (CH_2), 64.08 (CH_2), 64.23 (CH_2), 68.14 (CH_2), 114.97 (CH), 121.38 (CH), 126.56 (CH), 127.62 (C), 127.72 (CH), 128.38 (CH), 128.43 (CH), 128.45 (CH), 129.32 (CH), 129.62 (CH), 130.68 (C), 130.75 (CH_2), 131.98 (C), 140.35 (C), 145.88 (C), 148.50 (C), 148.91 (C), 159.56 (C), 165.31 (C), 166.65 (C). Anal. Calcd for $C_{45}H_{52}O_7$ (704.87): C, 76.67; H, 7.44. Found: C, 76.59; H, 7.41.

Bis[4-[(6*R*)-6-cyano-7-[4-(*tert*-butoxycarbonyl)phenyl]heptyl]-phenyl] 4,4′-Biphenyldicarboxylic Ester (13). To a suspension of **3** (0.81 g, 2.05 mmol), 4,4′-biphenyldicarboxylic acid (1.5 g, 6.15 mmol), and DPTS (300 mg) in dichloromethane (32 mL) was added DIPC (1.07 mL, 6.8 mmol) under nitrogen atmosphere. The mixture was stirred at room temperature for 48 h, and the solid precipitates (urea and 4,4′-biphenylcarboxylic acid) were removed by vacuum filtration. After drying ($MgSO_4$) and concentration, the residue was purified by flash chromatography using dichloromethane as eluent. The product was further purified by recrystallization from a mixture of dichloromethane and methanol to give 0.92 g (89.9%) of product **13** as a white solid: ^{1}H NMR (300 MHz, $CDCl_3$, TMS) δ 1.3−1.8 (m, 16H), 2.63 (t, J = 7.61 Hz, 4H), 2.7−2.8 (m, 2H), 2.8−3.0 (m, 4H), 7.15 (d, J = 8.39 Hz, 4H), 7.23 (d, J = 8.55 Hz, 4H), 7.29 (d, J = 8.18 Hz, 4H), 7.78 (d, J = 8.37 Hz, 4H), 7.97 (d, J = 8.13 Hz, 4 H), 8.30 (d, J = 8.32 Hz, 4H); ^{13}C NMR (75 MHz) δ 26.82 (CH_2), 28.05 (CH_3), 28.39 (CH_2), 30.90 (CH_2), 31.55 (CH_2), 33.36 (CH), 34.97 (CH_2), 38.10 (CH_2), 80.87 (C), 121.27 (CH), 127.33 (C), 128.76 (CH), 129.13 (CH), 129.23 (CH), 129.72 (CH), 130.67 (CH), 130.89 (C), 139.89 (C), 141.51 (C), 144.62 (C), 148.75 (C), 164.82 (C), 165.28 (C). Anal. Calcd for $C_{64}H_{68}O_8N_2$ (993.20): C, 77.39; H, 6.8; N, 2.82. Found: C, 77.32; H, 6.93; N, 2.82.

Characterization. Transmission electron microscopy (TEM) and electron diffraction utilized a Philips EM 420 electron microscope operated at 120 kV. TEM samples were prepared as very thin films (<1000 Å) cast from dilute chloroform solution on a glycerin surface. These films were rinsed several times in distilled water and then placed on 3 mm diameter copper grids. Prior to examination of images in the electron microscope, samples were shadowed with platinum and carbon to enhance image contrast. The camera length was calibrated using TlCl evaporated on the samples. Differential scanning calorimetry (DSC) was carried out in Perkin Elmer DSC-4 calorimeter. Samples for DSC ranged from 3 to 5 mg and were encapsulated in a standard aluminum pan. Gel permeation chromatography utilized a Waters 600E instrument and tetrahydrofuran as the solvent of experimental samples. Infrared and NMR spectra were obtained using a GE QE 300 instrument and an IBM IR/32 FTIR spectrometer, respectively.

Acknowledgment. This work was supported by Grant DMR-9312601 from the National Science Foundation. The electron microscopy and the diffraction work were carried out in the Center for Microanalysis of Materials, University of Illinois, which is supported by the U.S. Department of Energy under Grant DEFG02-91-ER45439.

JA9425851